Dear Editor, Atmospheric, Chemistry and Physics Discussion:

Please find below our item-by-item response to the Reviewer's comments regarding manuscript ***"Quantifying the sensitivity of aerosol optical properties to the parameterizations of physico-chemical processes during the 2010 Russian wildfires and heatwave"*** *by L. Palacios-Peña et al.*

Do not hesitate to contact us with further questions.

With kind regards,

Laura Palacios Peña

First of all, we would gratefully thank all the Editor and Reviewers for their valuable comments on the manuscript.

Anonymous Referee #1:

Q: My main concern with this study is related to the comparability of the different sensitivity tests. For example, RH is changed by -10 %, +0.5 %, and +1 %, whereas dry deposition velocity is scaled by 0.5 and 2 for the Aitken mode and 0.1 and 10 for the accumulation mode. As these changes vary from 0.5 % to 1000 % it is quite hard to understand how these sensitivity tests compare with each other. And why didn't you simulate RH reduction of 1 % and 0.5 %? Then they could have been compared directly with the enhancements. I think, it would be good to explain in the text why these changes are thought to be representative, meaningful and comparable for the parameters. For example, do they represent similar portions of the total ranges of the parameters? Or do they map the uncertainty ranges of these parameters? In order to say that sensitivity of the optical properties to RH is more important than to dry deposition, the changes in the parameters should be somehow comparable. This could be the true for current the analysis but it is not clear to the reader.

A: Following both reviewer suggestions, the section 2.3 "Sensitivity test" has revised and the explanation of the reasons for the selection of the ranges of the parameters has been expanded.

"RH […] In order to avoid unlikely supersaturation values (higher than 1%) the chosen upper values were 1.005 and 1.01; that is, 0.5% and 1% supersaturation respectively. However, these variations would be irrelevant in the opposite direction (-0.5 and -1%). Because of that and following the evaluation of this meteorological variable conducted by Tucella et al. (2012) and Zabkar et al. (2015), this variable was scaled to 0.9 (a reduction of 10%).

[…] The modification for our sensitivity test regarding dry deposition consists on scaled DDV by the values indicated in Table~1. Following Lee et al. (2013), DDV has been scaled to 0.5 and 2 for the Aitken mode and 0.1 and 10 for the Accumulation mode, which are the both ends of the uncertainty range of these parameters. […].

[…] sub-grid convective transport […] Following the evaluations carried out by Doherty et al. (2005) and Quan et al. (2016), the output temporal tendency has been scaled to ±50%. […]"

The following Table indicates the responses of the different simulations to the variations specified. As seen on the Table, the sensitivity experiments have been selected so that they lead to analogous maximum modifications of AOD.

Table 1. Key processes of the sensitivity tests and their variation. The maximum AOD response to these variations is indicated in the last column.

Process	*Sensitivity variation*	*Relative sensitivity variation*	*MAX AOD variation*
L10RH	**0,9*	*10%*	*0,6*
H05RH	**1,05*	*0.5%*	*< 0,15*
H1RH	**1,1*	*1%*	*0,2*
NO_DD	*OFF*	*100%*	*0,35*
LDDV_AIT	**0,5*	*50%*	*0,3*
HDDV_AIT	**2*	*100%*	*0,3*
LDDV_ACC	**0,1*	*90%*	*0,3*
HDDV_ACC	**10*	*1000%*	*0,3*
NO_CONV_TR	*OFF*	*100%*	*0,4*
HCONV_TR	**0,5*	*50%*	*0,4*
LCONV_TR	**1,5*	*50%*	*0,4*
NO_WS	*OFF*	*100%*	*0,2*

Q: […] Could you please clarify in the text if the conclusions are limited to specific conditions or if there are other processes which might have a stronger effect in some conditions.

A: A new section has been included where the limitations of this study are discussed highlighting other sources of errors and the extent of the conclusions due to focus only one episode. More details are explained in the next reply.

Q: I would have also liked to see a bit more detailed discussion on the significance of these results. Lately, there have been some studies where identical anthropogenic aerosol fields have been used in different models. For example, Nordling et al. (2019) found significant differences in the aerosol

forcing between the models and they concluded that differences in model circulation responses appear to dominate the differences in regional climate responses. So, I feel that it would be an interesting addition to discuss (and compare at some level) the significance of the processes analyzed in this manuscript and uncertainties in simulated circulation.

A: As both reviewers suggested a new section with an extensive discussion of the results regarding other processes, regions, periods and/ or conditions has been included in the manuscript.

"The main finding of this work is the non-linear response exhibited by AOD to the sensitivity of different key processes. This response is highly dependent on the thermodynamics equilibrium sulphate-nitrate-SOA, in which also water and ammonia operate. Moreover, and probably due to the nature of this episode, SOA shows a high impact on aerosol optical properties representation which was also found by Regayre et al., 2018 and Yoshioka, et al., 2019. These works highlighted a large uncertainty in effective radiative forcing due to ARI because of carbonaceous aerosols in high-emission months and in regions close to emission sources. However, under other conditions, the global influence of anthropogenic sulphate aerosol (not only due to emission but also to transport or lifetime; Kasoar et al., 2016; Regayre et al.,2018; Yoshioka et al., 2019); and in lesser extended nitrate (Balzarini et al., 2015); presented a significant influence on AOD estimations. Thus, a large effort should be devoted to the process understanding of this non-linear response from different key sources (RH, convective transport, dry deposition and likely other aerosol processes) and the improvement of representation of the sulphate-nitrate-ammonia-water equilibrium in models for a reduction in aerosol uncertainty.

From a global point of view, different works found the processes evaluated in this work to be important sources of uncertainty when characterizing aerosol optical properties and/ or radiative forcing (which is highly influenced by the latter). Regayre et al. (2018) found the deposition rate of aerosols and aerosol precursors (gases) to be the most important causes of the uncertainty related to effective radiative forcing. Also, dry deposition was the most important process for global mean CCN uncertainty (Lee et al., 2013), a source of uncertainty in AOD representation (Romakkaniemi et al. 2012). Although this process presents large uncertainties in AOD estimation in the aforementioned work, its importance is limited over a fire-affected region. Thus, attention should be taken in the evaluation of the uncertainty of this process depending on the scale, since likely the impacts of this process would be stronger over other regions, making it important globally. As was pointed out by Regayre et al., 2018 some uncertainty causes in radiative forcing could be because they cause at least a small amount of uncertainty in nearly all regions or because they are the largest

causes in some regions. Both Lee et al. (2013) and Regayre et al. (2018) used global model (GLOMAP-mode within the TOMCAT global 3-D offline chemistry transport model and HadGEM-UKCA model, respectively) during a whole year. Moreover, it should be highlighted that CCN uncertainty affects not only AOD representation but also to radiative forcing uncertainties due to ACI (Lee et a., 2013).

Similar results were found by Kipling et al. (2016) but for convective transport using the HadGEM3-UKCA model. This process was found to be very important in controlling the vertical profile of all aerosol components by mass. In addition, previous works as Palacios-Peña et al. (2018) and Palacios-Peña et al. (2019a) found that a misrepresentation of aerosol vertical profile could lead to uncertainties in the representation of AOD. On the other hand, Croft et al. (2012) evaluated the uncertainty due to different assumptions for the wet scavenging of aerosol and found a 20 to 35 % uncertainty in simulated global, annual mean AOD using the ECAM5-HAM model. However, the findings in our work regarding wet scavenging were lower due to the type of episode selected (without extensive clouds).

Another source of uncertainty is that related with general circulation. In this sense, Nordling et al. (2019) demonstrated a significant uncertainty in regional climate responses due to differences in circulation even with perfect aerosol descriptions. In addition, Brunner et al. (2015) pointed out the need for improving the simulations of meteorological parameters relevant for air quality. On the other hand, other works found an effect on meteorological variables, and thus, in circulation responses when aerosol effects are taken into account. This source of error is more relevant during the summer and near large sources of pollution (Makar et al., 2015; Baró et al., 2016), conditions that are similar to the episode analyzed here. These works show an impact on shortwave downwelling radiation at the surface, temperature, RH and PBL height due to the inclusion of aerosol effects which again could affect AOD uncertainties. Moreover, Kong et al. (2015) evidenced an improvement in the skill of meteorological variables when aerosol radiation effects were included. Thus, the uncertainties in the representation of the vertical distribution of aerosols and their optical properties revealed in this work could be limited to the influence of the regional circulation response, which in turn could again impact the aerosol distribution. Because of that, a reduction in this aerosol uncertainty could reduce the uncertainty in circulation response and thus, the evaluation of uncertainty could be constrained only to uncertainties in circulations mechanisms, as pointed out by Nordling et al. (2019).

Other important sources of uncertainty in aerosol optical properties representation among those evaluated here are the aerosol emissions (Granier

et al., 2011, Soares et al., 2015), representations of complex sub-grid processes (Weigum et al., 2016), aerosol processes (Croft et al., 2012), subsequent feedbacks on atmospheric dynamics (Bollasina et al., 2013; Booth et al., 2012; Villarini and Vecchi, 2013; Makar et al., 2015 and Baró et al., 2016; Norlding et al., 2019; Palacios-Peña et al., 2019b), aerosol mixing (Zhang et al., 2012; Curci et al., 2019) and aerosol size distribution (Tegen and Lacis, 1996; Claquin et al., 1998; Eck et al., 1999; Haywood and Boucher, 2000; Romakkaniemi et al., 2012; Obiso et al., 2017; Obiso and Jorba, 2018; Palacios-Peña et al., 2020). Another source of uncertainty is the choice of the aerosol-chemical mechanisms which was pointed out by Balzarini et al. (2015) and Palacios-Peña et al. (2018, 2019a).

In order to simplify the approach this study has been conducted using only one model; however, differences among models and how these represent the life cycle of aerosols should be kept in mind (Randles et al., 2013; Kim et al., 2014; Mann et al., 2014; Tsigaridis et al., 2014; Lacagnina et al., 2015; Pan et al., 2015; Ghan et al., 2016; Kipling et al., 2016; Koffi et al., 2016; Palacios-Peña et al., 2018, 2019a; Nordling et al., 2019) and similar studies with other model approach are necessary for an overall knowledge of these uncertainties."

Q: Page 1, lines 10-11: Are these absolute or relative differences. Would be good to clarify.

A: They are absolute differences. This has been clarified in the text.

Q: Page 2, line 23: "larger uncertainty", larger than what? Please, clarify.

A: This uncertainty is larger than for any other climate forcing agents. This has been clarified in the text. […] "one of the forcing agents with the largest uncertainty in the climate system"

Q: Page 2, line 33: "as aerosol optical properties" → such as aerosol optical properties. Can optical properties be considered as a process?

A: The reviewer is right; this sentence could lead to a misunderstanding. Because of that, the sentence has been rewritten as follow: "Numerical models are useful tools for understanding the different parameters influencing the atmospheric system, such as aerosol optical properties."

Q: Page 2, line 47: "high" → highly. A: Corrected

Q: Page 3, line 80: "To achieve this objective", it is not entirely clear what is objective you are referring to. A: This sentence has been rewritten in order to clarify the text.

Q: Page 3, line 83: What are the wavelengths of the AOD, extinction and backscatter coefficients? Please, mention them in the text.

A: Added

Q: Page 4, line 89: This sentence is a bit confusing: "with monthly mean temperatures in the summer months 5–9°C higher than those for 2002–2009 due to a prolonged blocking anticyclone situation which triggered large wildfires". First of all, I'm not sure what you mean with the temperature comparison. Were the monthly mean temperatures 5-9 degrees warmer than the monthly averages for 2002-2009 or was the comparison done for individual months and the temperature range covers all these months? Secondly, I don't think it was the anticyclone situation which triggered the fires. I believe it was the people and the meteorological situation just made the thing worse.

A: We mean that the monthly mean temperatures 5-9 degrees warmer than the monthly averages for 2002-2009. In order to clarify the meaning, this sentence has been rewritten as follow: "with a prolonged blocking anticyclone situation which favored an increase of the summer temperature (close to 9 degrees larger than 2002-2009 summers) promoting to larger wildfires"

Q: Page 4, line 107: I wouldn't call 0.95 a very high single-scattering albedo as sulphate aerosols have SSA close to unity. Or do you mean that the SSA was high for smoke aerosols?

A: The adjective very high has been removal in order to avoid misunderstandings.

Q: Page 4, line 116: There seems to be something missing from the end of the sentence ("in the"). Also, the unit should be Wm-2.

A: The reviewer was right. Both typos have been corrected.

Q: Page 5, line 142: Temporal profile of what? It seems that this sentence is missing some words.

A: Temporal profile of emission. The sentence has been rewritten in order to clarify this point.

Q: Page 6, line 156: "as nucleation, chemistry or uptake of water" → such as nucleation, chemistry and uptake of water

A: Corrected

Q: Page 7, line 193: Is the modelled AOD in Figure 2 an average over the studied period? I'm just wondering if an average is the best way to present the data as there was a lot of variability in AOD during the episode and single outliers can have a big impact on averages. Did you check how the results would look if you would use medians instead of averages? It would also be interesting to see the variability of AOD during the period. It is likely higher in the MAX-AOD and Moscow points than in the MIN-AOD point, which might have an effect on the differences between the studied points.

A:

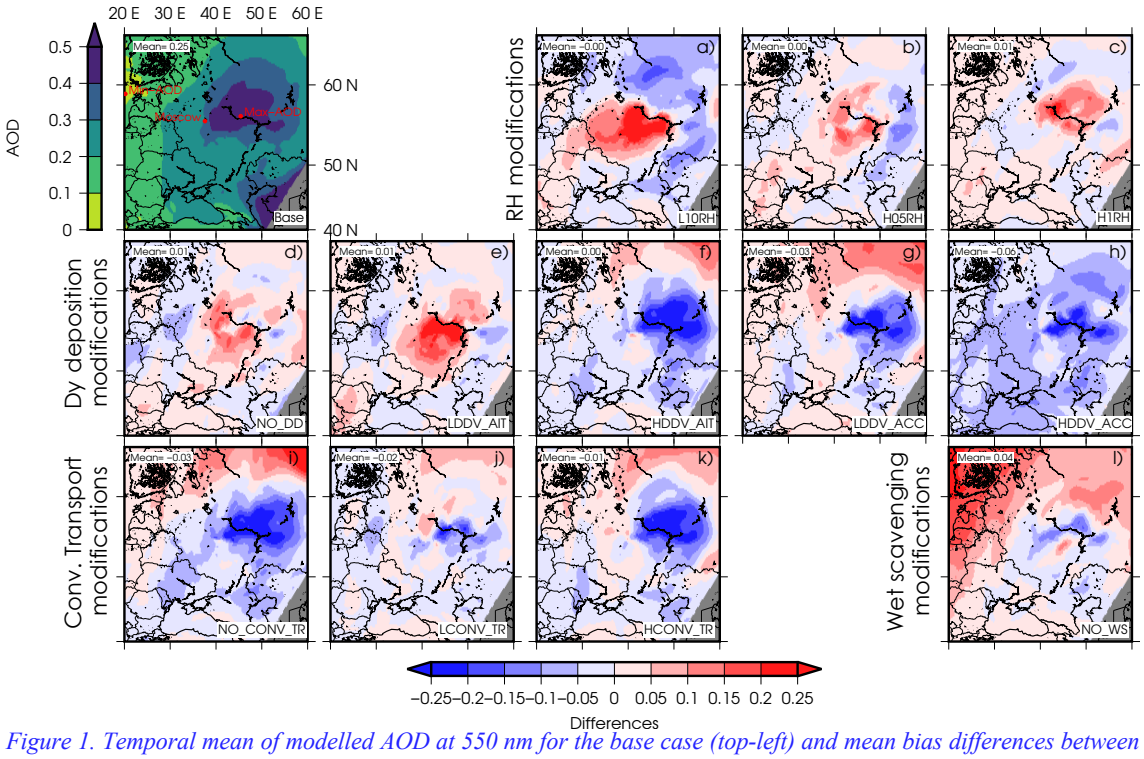

Figure 1. Temporal mean of modelled AOD at 550 nm for the base case (top-left) and mean bias differences between experiments and the base case.

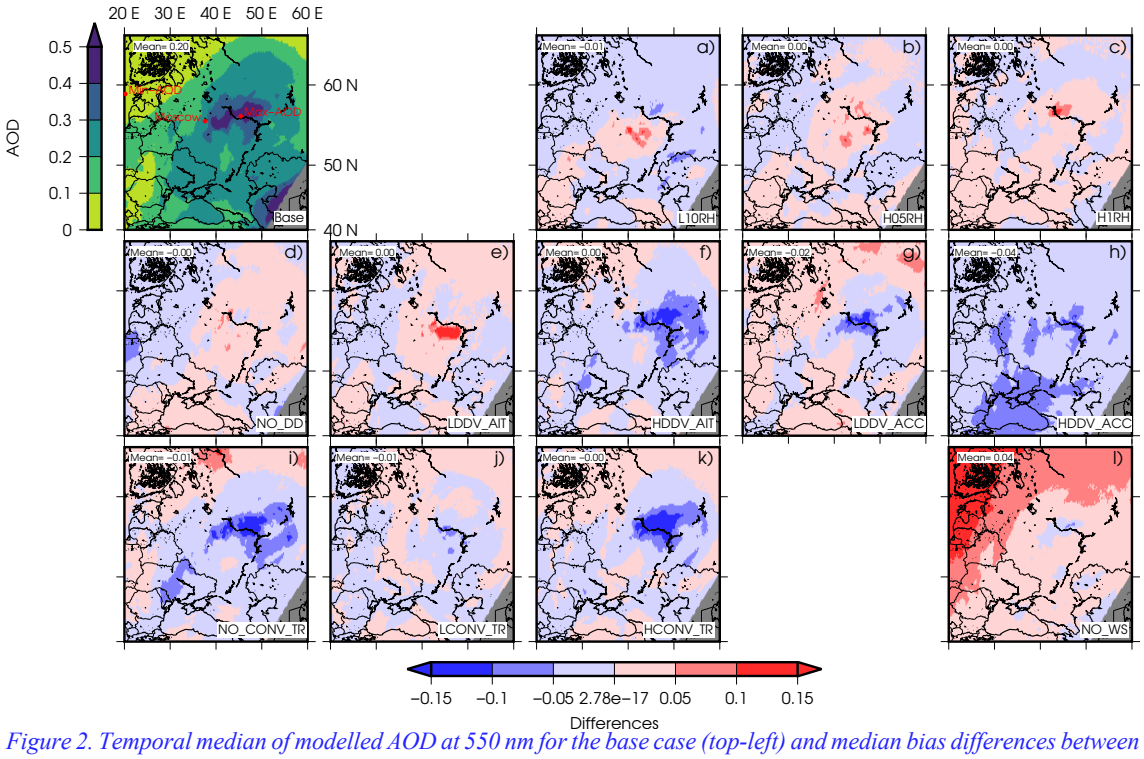

Figure 2. Temporal median of modelled AOD at 550 nm for the base case (top-left) and median bias differences between experiments and the base case

These figures show the temporal mean and the differences (top) and the temporal median and the temporal median of the differences (bottom). Figures reveal that for both, AOD and differences, the use of the temporal median displays similar results but less intense.

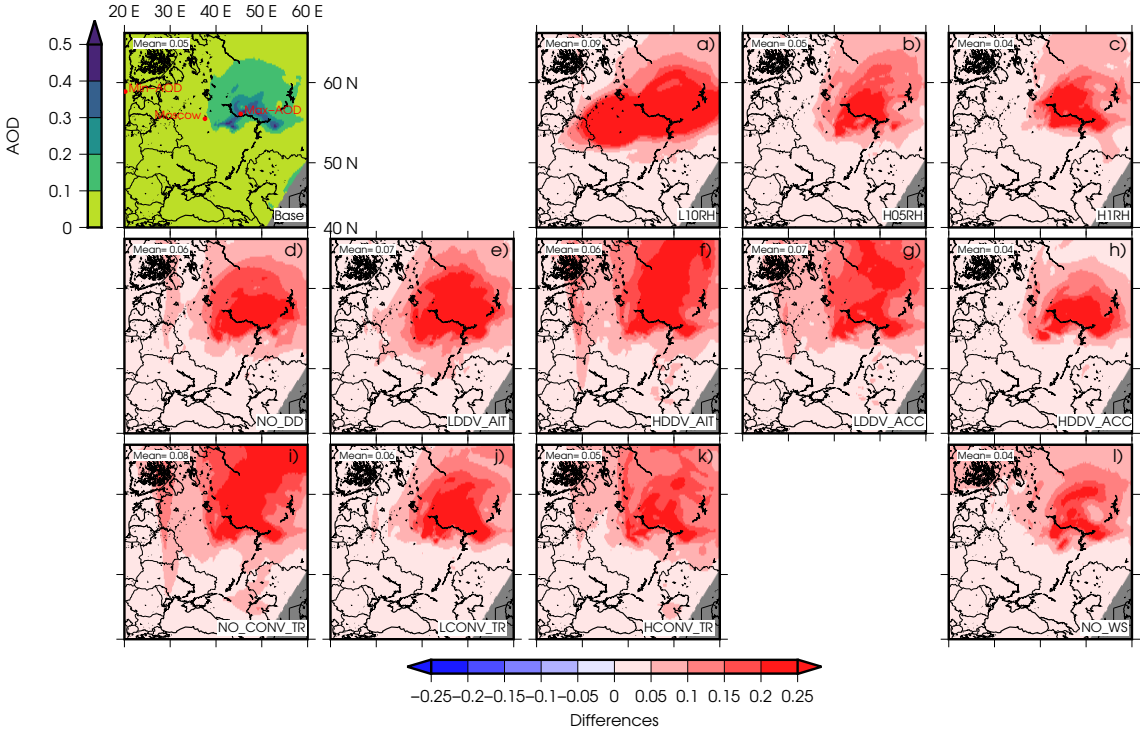

Figure 3. Temporal variability of modelled AOD at 550 nm for the base case (top-left) and temporal variability of the differences between experiments and the base case

Temporal variability is shown in the above figure. The reviewer suggested that the largest differences over the MAX-AOD locations are due to its high temporal variability meanwhile the small differences over the MIN-AOD location are due to its small temporal variability. However, according to the figure, temporal variability over the MOSCOW and MIN-AOD locations is similar meanwhile our results show higher impacts of the sensitivity test over the MOSCOW location.

Q: Page 7, line 194: "The top-right figure shows the mean bias ", do you mean the text in the top-left corner of the plots?

A: This sentence has been removed. This was a wrong sentence from an older version of the manuscript.

Q: Page 7, line 208; "but less significant", compared to what? I'm surprised that there isn't more discussion on the HDDV_ACC simulation as it produces the largest mean change in AOD (-0.06).

A: This sentence has been rewritten for the sake of clarification: "All the experiments related to changes in dry deposition (Figure 2,d-h) showed its strongest response located over the wildfires area, but this response is less relevant than for other cases." Moreover, a brief discussion of the HDDV_ACC test has been included: "HDDV_ACC is the only test which produces a general reduction in AOD over most of the study area (temporal and spatial mean change in AOD of -0.06) but this differences are stronger over fire affected areas and downwind."

Q: Page 7, line 213 and 216: The indices of the subplots seem to have been mixed: Figure 2, j → Figure 2, k, Figure 2, k → Figure 2, j

A: Corrected

Q: Page 8, line 217: What do you mean with smooth differences? Please clarify.

A: What smooth differences means is that differences in the LCONV_TRANS are lower in absolute terms. We try to clarify this point with this new sentence: "Figure 2,j indicates that the Low sub-grid Convective Transport case (LCONV_TR) has lower absolute differences are lower."

Q: Page 8, line 220: Here you could also mention that the mean AOD difference (0.04) for this simulation is the second largest even though there aren't many clouds in the studied domain. It implies that the wet scavenging is really important when there are clouds present.

A: We thanks the reviewer for its valuable comment. This has been included in the section 3.1.

Q: Page 8, line 224: "where the spot where" → the spots where. "claims to bring" → aims to bring

A: Corrected

Q: Page 8, line 225: "time mean" → temporal mean

A: Corrected

Q: Page 8, line 228: Please clarify in the text that these are profiles are temporal averages. Would the results look the same if medians were used instead of averages?

A: This has been clarified in the text. Regarding the use of the medians, the median of modelled AOD for the base case is shown above. This figure indicates that median AOD values are a bit lower that mean AOD values. However, the spatial pattern is similar for both, median and mean. Consequently, using the median instead of the mean does not change the conclusion obtained for the vertical profiles.

Q: Page 8, line 230: "α and β present similar profiles" sounds a bit strange to me. Do you mean that the profiles of "α and β have similar shapes?

A: The reviewer is right. This has been corrected

Q: Page 8, line 232: This and the following sentence are missing "for β" after the backscatter values.

A: Added

Q: Page 8, line 245: These low LR values are a surprising and interesting result. Especially, as the LR values over the MIN-AOD location are in the same range as reported by Mielonen et al. (2013). What could explain the large difference in the source and reasonable results farther away? I believe this would be an interesting point to discuss in the manuscript.

A: LR values over the MIN-AOD location are not comparable to those values reported by Mielonen et al. (2013) because these latter were reported over biomass burning affected areas. Over the MIN-AOD location, sea salt is predominant. Over this location LR values expected should be close to 30 sr^{-1}. Moreover, extinction and backscatter modelling profiles shape are similar, which

is not similar to most of the observed profiles, resulting in a misrepresentation of the LR. This could be ascribed to the model estimation of these aerosol optical properties profiles.

This clarification has been included in the text. Page 9, line 256: "[…] It is noticeable that LR values over the MIN-AOD location (close to 30 sr^{1}) are not comparable to those values expected by the scientific literature (e.g. Mielonen et al., 2013). However, it should be born in mind that MIN-AOD location is affected principally by sea salt, while the aforementioned reference covers a biomass-burning affected area. Moreover, extinction and backscatter modelling profiles shape are similar (rather constant at levels close to the surface), which is not found in most of the observed LR profiles. This could be ascribed to a model misrepresentation of extinction and backscatter modelling profiles. […]"

Q: Page 9, line 251: Please, clarify in the text how you calculated the mean absolute error for the profiles in practice. Did you first calculate the errors for each model level and then average them for the whole profile?

Page 9, line 252: I didn't quite catch how you calculated the normalized error. Could you please clarify? Which values were used in the normalization and how was it done in practice? Did you use the pixel-wise mean values from the base case at each model level or averaged over the whole column?

A: Both, the mean absolute error (MAE) and the normalize MAE (NMAE) were estimated by computing the error at each model level and then averaging along the whole profile. Regarding NMAE, as indicated in the manuscript, it was normalized dividing by the base case at each level. The objective was to show the magnitude of the relative changes in each sensitivity test for each evaluated variable. The two statistics were computed as follows:

$$MAE = \frac{\sum_1^n |x_{test} - x_{base}|}{n}$$

$$NMAE = \frac{\sum_1^n \frac{|x_{test} - x_{base}|}{x_{base}} x100}{n}$$

where n is the number of levels and x is the evaluated magnitude for the sensitivity test (x_{test}) and the base experiment (x_{base}).

To clarify the estimation of these two statistics, the manuscript has been rewritten: "In addition, Figures 4, 6 and 8 quantify the mean absolute error (MAE) of each experiment with respect to the base case, and in colors, the normalized MAE (NMAE). MAE has been estimated by averaging the absolute error of each

experiment regarding the base case at each model level. NMAE is the absolute error divided by the base case at each level and then averaged along the column. The NMAE analysis illustrates the relative change of each magnitude and helps to the intercomparison between the sensitivity test."

Q: Page 9, line 262: "optical properties profiles" → profiles of extinction and backscatter coefficients

A: Corrected

Q: Page 9, line 277: "However, in the case with a reduction of the RH in a 10 % (L10RH), NO^{-3} displays a similar concentration as the base case at surface levels and higher at levels above 800 hPa.", to me it seemed that the concentrations were similar only at surface levels and around 800 hPa. Did I read the figure wrong?

A: The reviewer is right, and this sentence has been rewritten for the sake of clarity. "However, in the case with a reduction of the RH in a 10% (L10RH), NO^{-3} displays a similar concentration as the base case at the surface level and around 800 hPa. Throughout the rest of the profile concentration is higher than in the base case but not as higher as in the H1RH case."

Q: Page 10, line 288: "hidroxy" → hydroxy

A: Corrected

Q: Page 10, line 294: "the shape of the NOx and SOA profiles are similar, and thus, at these vertical levels, variations in SOA concentrations may be due to the effect described by Sarrafzadeh et al. (2016): an increase in NOx concentrations at low-NOx conditions (less than 30 ppb or around 55 μg m−3)", this is a bit hard to follow. Would something like this work better: the shape of the NOx and SOA profiles are similar, and thus, at these vertical levels, variations in SOA concentrations may be due to an increase in NOx concentrations at low-NOx conditions (less than 30 ppb or around 55μg m−3; Sarrafzadeh et al. (2016))

A: The sentence has been rewritten as in the reviewer's suggestion.

Q: Page 10, line 297: "meanwhile in the L10RH case the positive variation of the concentration of SOA caused by the RH is limited.", I'm not sure what you mean with this. Could you please clarify?

A: As in the L10RH case there is not strong increase in NO_x the variation in SOA concentration cannot be highly dependent of the oxidation process described below and dependency of RH modification is higher. This has been clarified in

the text as: "That means that this variation depends more of RH modifications than NO_x oxidations".

Q: Page 10, line 300: "provokes" → provoke

A: Corrected

Q: Page 10, line 309: With "target area" you mean the MAX-AOD point? I find it interesting that in this NO_DD simulation the positive AOD change forms a similar arch as in the H05RH simulation whereas other simulations exhibit a more uniform blob around the MAX-AOD point (see Figure 2). Furthermore, the lowest values in the NO_WS simulation match approximately the "gap" in the blobs of the NO_DD and H05RH simulations. Could some specific process explain these common features in these simulations? Also, in this NO_DD simulation the AOD increased a lot more around the MAX-AOD point so would the conclusions have changed if the selected point would have been a bit more eastward (see Figure 2)? Based on the AOD changes shown in Figure 2, moving the point slightly eastwards would not affect the magnitude of the change much in most simulations. Maybe doing the profile analysis with averages calculated over a number of pixels would give more robust results as the AOD changes in all the simulation are not smooth around the MAX-AOD and Moscow points?

A: Yes, the target area means here the MAX-AOD location. This has been clarified in the text.

Regarding the blobs of the NO_DD and H05RH simulations, although the bias patterns of NO_DD and H05RH could share some similarities, it is difficult to attribute them to a specific process since the both present a low signal. The orography may play a relevant role. In some experiments, positive bias is concentrated on left of the Volga valley and negative bias is on the right. The arch seems to follow the river path shape, but it is difficult to extract a robust conclusion.

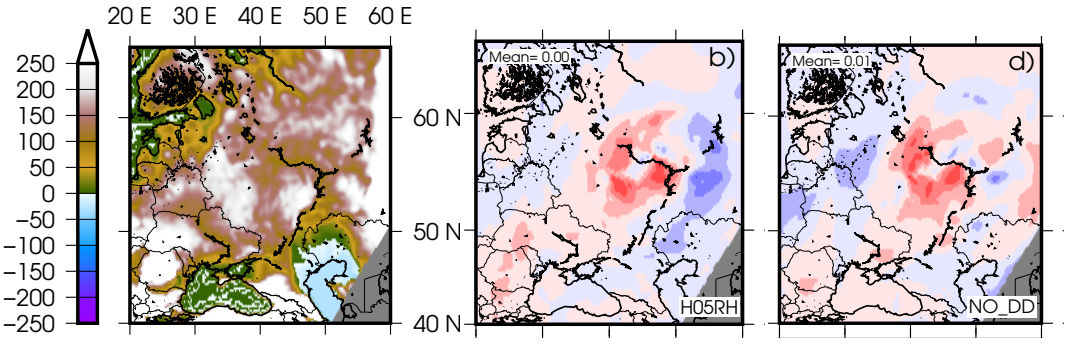

Figure 4. Terrain height in meters (left) and AOD differences between H05RH and NO_DD cases and the base case.

The selection of the most representative grid point to validate a simulation is always controversial. We agree that a common practice is making interpolations using several grid points in order to take into account the smoother orography always provided by a model. However, this approach does not always guarantee a better mismatch. Moreover, there are several methods of grid interpolations (bicubic, biquadratic), and using an interpolation approach to validate the simulation could be another source of uncertainty. The selection of the most suitable approach is out of the scope of this work. In our opinion, choosing the nearest neighbor facilitates the interpretation of the validation without tangle the results depending on the validation method.

Q: Page 10, line 315: Please note that Supplementary Figures 2 and 3 are not mentioned in the text at all.

A: Their references has been included in the text

Q: Page 10, line 316: "modifying the accumulation mode" → modifying the deposition of the accumulation mode. And the same change for the Aitken mode on the next line.

A: Added

Q: Page 11, line 327: "However, those species which are not directly emitted but are products of atmospheric chemistry (secondary aerosols), as SOA (NMAE>0.8 and MAE 0.2283) and most of the secondary inorganic species have their concentrations peak higher than those in the base case between 900 and 600 hPa", this sentence is hard to follow. Please, revise.

A: The sentence has been rewritten as follow: "However, secondary aerosol; which are not directly emitted and are products of atmospheric chemistry; such as SOA (NMAE>0.8 and MAE 0.2283) and most of the secondary inorganic species have their concentrations peak at a higher altitude than those in the base case between 900 and 600 hPa"

Q: Page 11, line 329: "fires area" → fire area, "optical properties profiles" → profiles of optical properties

A: Corrected

Q: Page 11, line 333: The Greenfield gap may not be familiar to all readers so, please, provide a size range and a reference for it.

A: As reviewer suggested this has been included in the text

Q: Page 11, line 340: "When the profiles are analyzed, the response differs between species. EC, POA and NO^{-3} shows a slight reduction in their concentration, and SOA exhibits a large reduction.", is this correct? Based on Figure 3, it seemed that the concentrations of NO^{-3} and SOA increased. Furthermore, the SEA concentration appeared to decrease and not increase as mentioned in the text and the highest SO_2^{-4} concentrations appear to be around 800 hPa, not near the surface. Did I read the figure correctly?

A: There is an error in the legend of the figure and the colors are changed. This has been corrected in the new figures.

Q: Page 11, line 348: "β profile is similar to the profiles of organic species (EC, POA and SOA)", to me it seems that the β profile is also similar to NH^{-4} and $SO2^{-4}$ profiles.

A: The reviewer is right. This sentence has been corrected.

Q: Page 12, line 358: "scaled to 1.5" → scaled by 1.5

A: Corrected

Q: Page 12, line 359: "For these species, the NO_CONV_TR experiment exhibits a concentration profile similar to the base case with slightly higher concentrations at surface levels and lower at higher levels", isn't it the opposite for the SEA concentrations? And the SOA, NO-3, and NH-4 concentrations appear to be constantly smaller than the base case? It would also be good to mention at the beginning of each section that which point is analyzed. I'm guessing this analysis is related to the MAX-AOD point.

A: The reviewer is right and this point has been clarified in the text as follows: "For POA, EC and SO4-2, the NO_CONV_TR experiment exhibits a concentration profile similar to the base case with slightly higher concentrations at surface levels and lower at higher levels. The opposite behavior is displayed

by SEA concentrations. Moreover, SOA, NO-3 and NH-4 concentration are constantly smaller than the base case."

The reviewer is right again, and the analyzed point is the MAX-AOD point. The text has been reviewed to clarify this somewhere was necessary.

Q: Page 12, line 369:" differantly as" → differently than

A: Corrected

Q: Page 12, line 376: "show a peak in their profiles around the PBL" → show a peak around the PBL

A: Corrected

Q: Page 12, line 382: "at surface levels" → at the lowest levels

A: Corrected

Q: Page 12, line 383: "below the PBL" → below 800 hPa

A: Corrected

Q: Page 12, line 384: "highlights the high impact of organic species", please, clarify this statement. The concentrations of inorganics over PBL are also decreased so why are organics are more important? Is it related to the higher mass of POA (max 150 μg m^{-3} vs. ~4 μg m^{-3})?

A: This is because the shape of the vertical profile of aerosol optical properties is quite similar to the shape of EC and POA. However, as the reviewer stated there is a reduction in the concentration of inorganics species and SOA over this location which could also impacts optical properties.

Q: Page 13, line 387: "experiment is that with the strongest" → experiment has the strongest

A: Corrected

Q: Page 13, line 391: "It should also be highlighted that over the MIN-AOD and Moscow spots, EC and POA profiles of the assessed experiments show larger differences between them than over the MAX-AOD. This fact could be explained because over these locations these species are not being directly emitted. Moreover, the farther the location is, the larger the differences are." This statement could be true in relative sense but what about in absolute values? The

concentration scales in the figures for the different locations are quite different. For example, the POA concentration scale is up to 150 μm m^{-3} at MAX-AOD, 30 μm m^{-3} at Moscow and only 2 μm m^{-3} at MIN-AOD. Therefore, based on figures 3, 5, 7 it is quite impossible to say which location has the largest changes in absolute sense. Could you please discuss this in more detail in the text?

A: What we mean with these differences was differences between the profile shape. Thus, the farther the location is the more different is the shape of the vertical profiles and this could be highly influenced by the transport processes. In order to clarify this statement, the paragraph has been rewritten as follows: "It should also be highlighted, the profile shape of EC and POA over the MIN-AOD and Moscow show larger differences than over the MAX-AOD area for the different experiments. These differences in the shape profiles could be attributed to these species are not directly emitted over MIN-AOD and Moscow areas and transport processes could be influenced by vertical distribution. Moreover, the farther the location is, the more different the shape of the vertical profile is."

Q: Page 13, line 397: "In order to reduce", please explain how the uncertainties can be reduced based on the results presented in this study.

A: This sentence has been rewritten in order to a better explanation: "This work assesses the sensitivity of aerosol optical properties and the aerosol vertical distribution to key physical processes. To achieve this objective, sensitivity runs modifying RH, dry deposition, sub-grid convective transport and wet scavenging have been carried out for the 2010 Russian heatwave/wildfires episode with the WRF-Chem regional fully coupled model. Findings in this work would help to improve modelling aerosol representation giving some initial guidelines about what parameters could be misrepresented or are the most sensitive to the vertical mixing."

Q: Page 13, line 400: "carried out during" → carried out for

A: Corrected

Q: Page 13, line 412: What do you mean with "important supersaturation"?

A: Supersaturation above 1% because supersaturation rarely exceeds 1%–2% and this only can be in warm clouds (Devenish et al.2016) in particular vigorous convective clouds (Prabha et al. 2011). This has been clarified in the text.

Q: Page 14, line 442: It would be good to mention in this paragraph that the simulated LR values were different only/mainly at the MAX-AOD location, not everywhere.

A: This has been clarified in the text as follows: "Regarding the LR, simulated values of this variable are remarkably different from those observed in the scientific literature, mainly over fire affected areas."

Q: Figure 2: Please, consider using binned color scale for the base AOD plot as well. Currently, the different hues are quite hard to differentiate. A binned color scale would make it easier to see the differences between the regions.

A: The figure has been redone as reviewer's suggestions

Q: Figures 3, 5, and 7: Currently the lines are quite hard separate from each other. Maybe thicker lines would make it easier to see the colors?

A: The figures have been redrawn as reviewer's suggestions

Q: Figures 4, 6, 8: Please, consider using binned color scale for the NMAE as it could make it easier to compare the different cases.

A: The figures have been redrawn as reviewer's suggestions

References:

Nordling, K., Korhonen, H., Räisänen, P., Alper, M. E., Uotila, P., O'Donnell, D., and Merikanto, J.: Role of climate model dynamics in estimated climate responses to anthropogenic aerosols, Atmos. Chem. Phys., 19, 9969–9987, https://doi.org/10.5194/acp-19-9969-2019, 2019.

Balzarini et al., (2015): WRF-Chem model sensitivity to chemical mechanisms choice in reconstructing aerosol optical properties, 115, 604-619, doi: 10.1016/j.atmosenv.2014.12.033

Baró et al., (2016): Biomass burning aerosol impact on surface winds during the 2010 Russian heat wave, 44, 2, doi: 10.1002/2016GL071484

Bollasina, et al., (2013), Earlier onset of the Indian monsoon in the late twentieth century: The role of anthropogenic aerosols, Geophys. Res. Lett., 40, 3715– 3720, doi:10.1002/grl.50719.

Booth et al., (2012): Aerosols implicated as a prime driver of twentieth-century North Atlantic climate variability. Nature 484, 228–232. https://doi.org/10.1038/nature10946

Brunner, D. et al., (2015): Comparative analysis of meteorological performance of coupled chemistry-meteorology models in the context of AQMEII

phase 2, Atmospheric Environment, 115, 470-498, doi: 10.1016/j.atmosenv.2014.12.032.

Claquin, T., et al.: Uncertainties in assessing radiative forcing by mineral dust, Tellus B, 50, 491 – 505, doi: 10.1034/j.1600-0889.1998.t01-2-00007.x, 1998.

Croft, B. et al., (2012): Uncertainty associated with convective wet removal of entrained aerosols in a global climate model, Atmos. Chem. Phys., 12, 10725–10748, https://doi.org/10.5194/acp-12-10725-2012, 2012.

Curci, G., et al.: Modelling black carbon absorption of solar radiation: combining external and internal mixing assumptions, Atmo- spheric Chemistry and Physics, 19, 181 – 204, doi: 10.5194/acp-19-181-2019, 2019.

Devenish, B.J., K. Furtado, and D.J. Thomson, 2016: Analytical Solutions of the Supersaturation Equation for a Warm Cloud. J. Atmos. Sci., 73, 3453–3465, https://doi.org/10.1175/JAS-D-15-0281.1

Eck, T. F., et al.: Wavelength dependence of the optical depth of biomass burning, urban, and desert dust aerosols, Journal of Geophysical Research: Atmospheres, 104, 31 333 – 31 349, doi: 10.1029/1999JD900923, 1999.

Ghan, S. J., et al.: Challenges in constraining anthropogenic aerosol effects on cloud radiative forcing using present-day spatiotemporal variability, Proc. Natl. Acad. Sci. USA, 113, 5804–5811, https://doi.org/10.1073/pnas.1514036113, 2016.

Granier, C. et al., (2011): Evolution of anthropogenic and biomass burning emissions of air pollutants at global and regional scales during the 1980–2010 period. Climatic Change 109, 163. https://doi.org/10.1007/s10584-011-0154-1

Haywood, J. and Boucher, O.: Estimates of the direct and indirect radiative forcing due to tropospheric aerosols: A review, Reviews of Geophysics, 38, 513 – 543, doi: 10.1029/1999RG000078, 2000.

Kasoar, M. et al., (2016): Regional and global temperature response to anthropogenic SO2 emissions from China in three climate models, Atmos. Chem. Phys., 16, 9785–9804, https://doi.org/10.5194/acp-16-9785-2016, 2016.

Kim, D., et al.: Sources, sinks and transatlantic transport of North African dust aerosol: A multimodel analysis and comparison with remote sensing data, J. Geophys. Res.-Atmos., 119, 6259–6277, https://doi.org/10.1002/2013JD021099, 2014.

Koffi, B., et al.: Evaluation of the aerosol vertical distribution in global aerosol models through comparison against CALIOP measurements: AeroCom phase II results, J. Geophys. Res.-Atmos., 121, 7254–7283, https://doi.org/10.1002/2015JD024639, 2016.

Kong et al., (2015): Analysis of meteorology–chemistry interactions during air pollution episodes using online coupled models within AQMEII phase-2, 115, 527-540, doi: j.atmosenv.2014.09.020

Lacagnina, C., et al.: Aerosol single-scattering albedo over the global oceans: Comapring PARASOL retrievals with AERONET, OMI, and AeroCom models estiamtes, J. Geophys. Res.-Atmos., 120, 9814–9836, https://doi.org/10.1002/2015JD023501, 2015.

Mann, G. W., et al.: Intercomparison and evaluation of global aerosol microphysical properties among AeroCom models of a range of complexity, Atmos. Chem. Phys., 14, 4679–4713, https://doi.org/10.5194/acp-14-4679-2014, 2014.

Makar et al., (2015): Feedbacks between air pollution and weather, Part 1: Effects on weather, 115, 442-469, doi: 10.1016/j.atmosenv.2014.12.003

Obiso, V. and Jorba, O.: Aerosol-radiation interaction in atmospheric models: Idealized sensitivity study of simulated short-wave direct radiative effects to particle microphysical properties, Journal of Aerosol Science, 115, 46 – 61, doi: 10.1016/j.jaerosci.2017.10.004, 2018.

Obiso, V., et al.: Impact of aerosol microphysical properties on mass scattering cross sections, Journal of Aerosol Science, 112, 68 – 82, doi: 10.1016/j.jaerosci.2017.03.001, 2017.

Palacios-Peña, L.et al.: An assessment of aerosol optical properties from remote-sensing observations and regional chemistry–climate coupled models over Europe, Atmos. Chem. Phys., 18, 5021–5043, https://doi.org/10.5194/acp-18-5021-2018, 2018.

Palacios-Peña, L., et al.: Aerosol optical properties over Europe: an evaluation of the AQMEII Phase 3 simulations against satellite observations, Atmos. Chem. Phys., 19, 2965–2990, https://doi.org/10.5194/acp-19-2965-2019, 2019a.

Palacios-Peña, L., et al.: Saharan Dust Modeling Over the Mediterranean Basin and Central Europe: Does the Resolution Matter?, Frontiers in Earth Science, 7, 290, doi: 10.3389/feart.2019.00290, 2019b.

Pan, X.,et al.: A multi-model evaluation of aerosols over South Asia: common problems and possible causes, Atmos. Chem. Phys., 15, 5903–5928, https://doi.org/10.5194/acp-15-5903-2015, 2015.

Prabha, T.V., et al., 2011: Microphysics of Premonsoon and Monsoon Clouds as Seen from In Situ Measurements during the Cloud Aerosol Interaction and Precipitation Enhancement Experiment (CAIPEEX). J. Atmos. Sci., 68, 1882–1901, https://doi.org/10.1175/2011JAS3707.1

Randles, C. A., et al.: Intercomparison of shortwave radiative transfer schemes in global aerosol modeling: results from the AeroCom Radiative Transfer Experiment, Atmos. Chem. Phys., 13, 2347–2379, https://doi.org/10.5194/acp-13-2347-2013, 2013.

Regayre, L. A. et al.: Aerosol and physical atmosphere model parameters are both important sources of uncertainty in aerosol ERF, Atmos. Chem. Phys., 18, 9975–10006, https://doi.org/10.5194/acp-18-9975-2018, 2018.

Romakkaniemi, S. et al.: Effect of aerosol size distribution changes on AOD, CCN and cloud droplet concentration: Case studies from Erfurt and Melpitz, Germany, Journal of Geophysical Research: Atmospheres, 117, D07 202, doi: 10.1029/2011JD017091, 2012.

Soares, J., et al.: Uncertainties of wild-land fires emission in AQMEII phase 2 case study, Atmospheric Environment, 115, 361 – 370, doi: 10.1016/j.atmosenv.2015.01.068, 2015.

Tegen, I. and Lacis, A. A.: Modeling of particle size distribution and its influence on the radiative properties of mineral dust aerosol, Journal of Geophysical Research: Atmospheres, 101, 19 237 – 19 244, doi: 10.1029/95JD03610, 1996.

Tsigaridis, K., et al.: The AeroCom evaluation and intercomparison of organic aerosol in global models, Atmos. Chem. Phys., 14, 10845–10895, https://doi.org/10.5194/acp-14-10845-2014, 2014.

Villarini, G. and G.A. Vecchi, 2013: Projected Increases in North Atlantic Tropical Cyclone Intensity from CMIP5 Models. J. Climate, *26, 3231–3240, https://doi.org/10.1175/JCLI-D-12-00441.1*

Weigum, N., et al.: Effect of aerosol subgrid variability on aerosol optical depth and cloud condensation nuclei: implications for global aerosol modelling, Atmos. Chem. Phys., 16, 13619–13639, https://doi.org/10.5194/acp-16-13619-2016, 2016.

Yoshioka, M. et al. (2019). Ensembles of global climate model variants designed for the quantification and constraint of uncertainty in aerosols and their radiative forcing. Journal of Advances in Modeling Earth Systems, 11, 3728– 3754. https://doi.org/10.1029/2019MS001628

Zhang, K., et al.: The global aerosol-climate model ECHAM-HAM, version 2: sensitivity to improvements in process representations, Atmospheric Chemistry and Physics, 12, 8911 – 8949, doi: 10.5194/acp-12-8911-2012, 2012.

Anonymous Referee #2:

General comments:

Q: 1/ In this paper, the authors chose to focus on the 2010 Russian heatwave/wildfires episode. However, I would have also liked to see a section dedicated to a scientific discussion including more references to previous works on the subject aiming other simulation periods, other regions affected by

wildfires ... in order to have wider conclusions and to highlight the significance of these results.

2/ The authors mentioned (only in the conclusion) that other processes (not discussed in their work) may also impact the aerosol optical properties representation. I believe that the paper could be further strengthened by adding a section in which the authors can compare their findings to more references that also discussed and analyzed the sensitivity of aerosol properties to other crucial parameters (such as, aerosol mixing state).

A: As both reviewers suggested a new section with an extensive discussion of the results regarding other processes, regions, periods and/ or conditions has been included in the manuscript. This discussion is in the response to reviewer #1.

Specific comments:

Q: 1/ Page 1, lines 10 -11: Please clarify if these differences are absolute or relative.

A: Differences are absolute. It has been clarified in the revised version of the manuscript.

Q: 2/ Page 3, lines 74-76: "The sensitivity tests were carried out using the WRF-Chem regional fully-coupled model by modifying dry deposition, sub-grid convective transport, relative humidity and wet scavenging." This sentence is repeated twice in the paper (here and in the abstract). Please formulate in a different way.

A: The sentence has been rewritten as follow: "This quantification has been estimated by sensitivity tests carried out using the WRF-Chem regional fully-coupled model. Modified aerosol processes and parameters are dry deposition, sub-grid convective transport, relative humidity and wet scavenging."

Q: 3/ Page 3, line 83: Please add the wavelengths at which the aerosol optical properties (AOD, extinction and backscatter coefficients) are calculated.

A: Added

Q: 4/ Page 5, lines 142-144: How these fire emissions are taken into account in the model? Can the authors give a brief description of the inventory and the uncertainties of the fire emissions used in this work?

A: The description of the fire emissions has been expanded as reviewer suggested. Moreover, a reference of the evaluation of this fire emission inventory has been provided.

"Biomass burning emission data of the total PM emissions (daily data with a spatial resolution of 0.1º) were derived from the project IS4FIRES (Integrated monitoring and modelling system for wild-land fires; Sofiev et al., 2009). As described by Soares et al., 2015 emissions were calculated from a re-analysis of the fire radiative power from MODIS on-board of Aqua and Terra satellites; and calibration emission factors based on the comparison between observations and modelled data processed by the System for Integrated modeLing of Atmospheric coMposition (SILAM). Day and night vertical injection profiles were also provided. Finally, total PM emissions were speciated to WRF-Chem emission species following Andreae and Merlet (2001) and Wiedinmyer et al. (2011). No heat release due to the fires was considered. Uncertainties were estimated by Soares et al.,2015 with an overestimation in-average of 20–30% which could raise to about 50% in specific episodes. This impacts on total emissions likely come from under-stated injection height which can lead to overestimation of the near-surface concentration and reduction of elevated plumes; or a misinterpretation by MODIS of oil and gas flares and large industrial installation as fires. More details can be found in Soares et al.,2015."

Q: 5/ Page 6, section 2.3: I think that the authors should better have two different sections: a section where they explain why they chose these "key sources" and another section where they describe the different sensitivity tests considered in their study.

A: Section 2.3 covers the definition of the sensitivity tests conducted in this contribution, while the key sources of uncertainty are profusely detailed in the introduction.

Q: 6/ Page 7, line 208; "...showed the strongest response located over the wildfires area, but less significant.", what do you mean here by "less significant"?

A: This sentence has been rewritten for the sake of clarification: "All the experiments related to changes in dry deposition (Figure 2,d-h) showed its strongest response located over the wildfires area, but this response is less relevant than for other cases."

Q: 7/ Page 7, line 194: "The top-right figure shows the mean bias ". Does the top-right figure in figure 2 shows the mean relative differences or the mean bias between experiments and the base case? Please clarify.

A: Figure 2 displays the mean bias between experiments and the base case. There was an error in the caption of the figure which has been corrected. The text has been checked in order to avoid similar errors.

Q: 8/ Page 8, line 229: What are these "SOA"?

A: SOA in this chemical mechanism are composed by SOA Anthropogenic and Biogenic organic, both dry and in cloud.

Q: 9/ Page 8, lines 228-229: Why did the authors evaluate only these species concentrations?

A: EC, POA and SOA were selected due to their importance in a biomass burning episode. NO3-, NH4- and SO2- have been selected because they are the main inorganic species and those involved in the sulphate-ammonium-nitrate-water equilibrium simulated by the ISORROPIA mechanism. Finally, SEA has been selected as an example of natural aerosol with a small impact on this episode. Dust concentrations are negligible over the target domain.

Q: 10/ Page 9, lines 251-252: How did the authors calculated the mean absolute error for the profiles? Can the authors add a definition of the statistical indicators used in their sensitivity study?

A: As we indicated in the response to the reviewer #1, a clarification of the estimation of these statistics has been added in the text.

Q: 11/ Page 10, line 315: Figures 2 and 3 in the supplementary material are not described or used in the text at all. Please add them.

A: A reference for these figures has been included in the text

Q: 12/ Page 11, line 333: What is the "Greenfield gap"? Please explain and add a reference.

A: As reviewer suggested this has been included in the text.

"(particle radii of the range of 0.1–1 μm where Brownian motion is not large anymore and gravitational settling is not yet important; Greenfield 1957; Ladino, et al. 2011)"

Q: 13/ Page 13, line 397: "In order to reduce (or, at least, quantify) this uncertainty ..." How can we use the findings of this paper to reduce uncertainties? Please explain.

A: This sentence has been rewritten in order to a better explanation: "This work assesses the sensitivity of aerosol optical properties and the aerosol vertical distribution to key physical processes. To achieve this objective, sensitivity runs modifying RH, dry deposition, sub-grid convective transport and wet scavenging have been carried out for the 2010 Russian heatwave/wildfires episode with the WRF-Chem regional fully coupled model. Findings in this work would help to improve modelling aerosol representation giving some initial guidelines about what parameters could be misrepresented or are the most sensitive to the vertical mixing."

Q: 14/ Page 13, line 409-410: Can the authors give more details about these papers' findings in order to highlight these similarities?

A: Following both reviewers suggestion this part of the manuscript has been rewritten including a comparison of our results with other similar studies.

Q: 15/ Page 14, line 422: what are these VOC?

A: VOC refers to Volatile organic compounds as described in page 10, line:XXX

Technical comments:

Q: 1/ Page 1, line 6: Please add a comma, after "In order to achieve this objective sensitivity".

A: Corrected

Q: 2/ Page 1, line 7 and Page 5, line 122: Please replace "fully coupled" by "fully-coupled".

A: Replaced

Q: 3/Page 2, line 23: Please correct "larger uncertainty" by "large uncertainty".

A: Corrected

Q: 4/ Page 2, line 47: "Please correct "high influenced" by "highly influenced".

A: Corrected

Q: 5/ Page 5, line 141: Please correct (PM_{10} ...).

A: Corrected

Q: 6/ Page 7, line 211: "provoke" please correct.

A: Corrected

Q: 7/Page 8, line 225: Please replace "time mean" by "temporal mean".

A: Corrected

Q: 8/ Page 10, line 288: "hydroxyl radical" please correct.

A: Corrected

Q: 9/ Page 10, line 300: "does not provoke" please correct.

A: Corrected

Q: 10/ Page 12, line 377: Please add a comma after "For the species, ..."

A: Corrected

Q: 11/ Page 16, References section: in the ACP journal, the name of the journals should be cited in abbreviations. Please correct.

A: The references section is automatically done by the Bibtex tool. I think this time of typos will be corrected during the edition process.

Q: 12/ Page 24, Figure 1: for the clearness of the figure, please fill the box (for the fire-affected target area) with a more transparent color.

A: Modified

References:

Andreae, M. O. and Merlet, P.: Emission of trace gases and aerosols from biomass burning, Global Biogeochemical Cycles, 15, 955 – 966, doi: 10.1029/2000GB001382, 2001.

Soares, J., Sofiev, M., and Hakkarainen, J.: Uncertainties of wild-land fires emission in AQMEII phase 2 case study, Atmospheric Environment, 115, 361 – 370, doi: 10.1016/j.atmosenv.2015.01.068, 2015.

Wiedinmyer, C., Akagi, S. K., Yokelson, R. J., Emmons, L. K., Al-Saadi, J. A., Orlando, J. J., and Soja, A. J.: The Fire INventory from NCAR (FINN): a high resolution global model to estimate the emissions from open burning, Geoscientific Model Development, 4, 625 – 641, doi: 10.5194/gmd-4-625-2011, 2011.

Quantifying the sensitivity of aerosol optical properties to the parameterizations of physico-chemical processes during the 2010 Russian wildfires and heatwave

Laura Palacios-Peña[1], Philip Stier[2], Raquel Lorente-Plazas[3], and Pedro Jiménez-Guerrero[1,4]

[1]Physics of the Earth, Regional Campus of International Excellence "Campus Mare Nostrum", University of Murcia, Spain.
[2]Atmospheric, Oceanic and Planetary Physics, Department of Physics, University of Oxford, UK.
[3]Dept. of Meteorology, Meteored, Almendricos, Spain.
[4]Biomedical Research Institute of Murcia (IMIB-Arrixaca), Spain.

Correspondence: Pedro Jiménez-Guerrero (pedro.jimenezguerrero@um.es)

Abstract. The impact of aerosol-radiation and aerosol-clouds interactions on the radiative forcing is subject to large uncertainties. This is caused by the limited understanding of aerosol optical properties and the role of aerosols as cloud condensation/ice nuclei (CCN/IN). On the other hand, aerosol optical properties and vertical distribution are highly related and their uncertainties come from different processes. This work attempts to quantify the sensitivity of aerosol optical properties (i.e. aerosol optical depth; AOD) and their vertical distribution (using the extinction coefficient, backscatter coefficient, and concentrations species profiles) to key processes. In order to achieve this objective, sensitivity tests have been carried out, using the WRF-Chem regional ~~fully coupled~~ fully-coupled model by modifying the dry deposition, sub-grid convective transport, relative humidity and wet scavenging. The 2010 Russian heatwave/wildfire episode has been selected as case study.

Results indicate that AOD is sensitive to these key processes in the following order of importance: 1) modification of relative humidity, causing AOD differences up to 0.6; 2) modification of vertical convection transport with AOD differences around -0.4; and 3) the dry deposition with AOD absolute differences up to -0.35 and 0.3. Moreover, these AOD changes exhibit a non-linear response. Both, an increase and a decrease in the RH result in higher AOD values. On the other hand, both, the increase and offset of the sub-grid convective transport lead to a reduction in the AOD over the fire area. In addition, a similar non-linear response is found when reducing the dry deposition velocity; in particular, for the accumulation mode where the concentration of several species increases (while a decrease might be expected). These non-linear responses are highly dependent on the equilibrium of the thermodynamics system sulphate-nitrate-SOA (secondary organic aerosol). In this sense, small changes in the concentration of one species can strongly affect others, finally affecting aerosol optical properties. Changes in this equilibrium could come from modifications in relative humidity, dry deposition or vertical convective transport. By itself, dry deposition also presents a high uncertainty influencing the AOD representation.

Copyright statement. TEXT

1 Introduction

Since the First Assessment Report of the Intergovernmental Panel on Climate Change (IPCC), a wide scientific consensus identifies atmospheric aerosols and clouds as one of the forcing agents with ~~a larger~~ the largest uncertainty in the climate system (Charlson et al., 1992; Schimel et al., 1996; Penner et al., 2001; Randall et al., 2007; Forster et al., 2007; Boucher, 2015). Atmospheric aerosols modify the Earth's radiative budget through aerosol-radiation interactions (ARI) and aerosol-cloud interactions (ACI). ARI lead to a redistribution of radiative energy in the atmosphere through scattering and absorption. In addition, ACI modify cloud microphysical properties and precipitation regimes as well as cloud effects on radiation (Randall et al., 2007; Boucher et al., 2013).

ARI and ACI are strongly dependent on aerosol optical properties and the ability of aerosols to act as cloud condensation nuclei (CCN) or ice nuclei (IN), which are controlled by the spatio-temporal aerosol distribution, the aerosol size, composition and mixing state (Stier et al., 2005). Thus, to determine and constrain the uncertainty in aerosol optical properties is a key issue for a better assessment of the uncertainty in aerosol effects.

Numerical models are useful tools for understanding the different ~~processes~~ parameters influencing the atmospheric system, such as aerosol optical properties. The complexity of how aerosols are treated in models varies widely, since these models take into account processes as emission, transport, deposition, microphysics and chemistry (Kipling et al., 2016). Differences in complexity primarily arise from representations of aerosol size distribution and mixing states. The most complex and realistic models are those considering the inclusion of ARI and ACI since they allow a fully-coupled interaction of aerosols, meteorology, radiation and chemistry. One example of these numerical models is WRF-Chem (Grell et al., 2005), used in this work. Notwithstanding the complexity of aerosol treatment in these models, there are still high uncertainties in processes representing the aerosol optical properties.

As stated by previous works ~~(e.g. Palacios-Peña et al. (2017, 2018, 2019a))~~(e.g. Palacios-Peña et al., 2017, 2018, 2019a), uncertainties in aerosol optical properties may be influenced by a number of factors, namely emissions; aerosol mass concentration; particle size representation (Balzarini et al., 2015); vertical distribution and location with respect to other forcing agents as clouds (Kipling et al., 2016); dry deposition and CCN (Romakkaniemi et al., 2012; Lee et al., 2013; Forkel et al., 2015); relative humidity (RH; Yoon and Kim, 2006; Zhang et al., 2012; Altaratz et al., 2013; Weigum et al., 2016); and aerosol internal mixing rules (Curci et al., 2019; Zhang et al., 2012).

Precisely, aerosol vertical distribution is ~~high~~ highly influenced by aerosol optical properties (Palacios-Peña et al., 2018, 2019a). Henceforth, Kipling et al. (2016) investigated the uncertainty in the vertical layering of aerosol particles to different parameters: convective transport, emissions injection and size; vertical advection, boundary-layer mixing, entrainment into convective plumes, condensation, coagulation, nucleation, aqueous chemistry, aging of insoluble particles, Aitken transition to accumulation mode, dry deposition, in-cloud and below-cloud scavenging and re-evaporation. The convective transport and the in-cloud scavenging were found to be very important when controlling the vertical profile of all-aerosol components by mass and those with the highest influence on aerosol optical depth ~~(AOD) (Kipling et al., 2016)~~(AOD; Kipling et al., 2016).

The representation of CCN has been also identified as another second-order source of uncertainty in aerosol optical properties, such as AOD. An increase in downward solar radiation was found by Forkel et al. (2015) and Romakkaniemi et al. (2012) when ACI were taken into account. This latter contribution found a relationship between a reduction in the AOD and CCN because the inclusion of ACI in numerical models leads to a reduction in CCN by the condensation kinetics of water during cloud droplet formation. This induces a reduction of the cloud droplet number, the cloud liquid water and, finally, an increase in downward solar radiation. In addition to AOD, CCN conditioned the uncertainty in ACI, as well as cloud occurrence and cloud-related processes (updraught speeds, precipitation processes, etc.). Because of that, the high uncertainty existing when modelling CCN was evaluated by Lee et al. (2013), finding that dry deposition was the most important process for this uncertainty over more than twenty-eight model parameters selected by expert elicitation, including nucleation, aerosol ageing, pH of cloud drops, nucleation scavenging, dry deposition, modal with mode separation diameter, emissions and production of secondary organic aerosols (SOA). These results, which are partly because wet deposition was not fully varied, were found in one model framework (with its own structural uncertainties).

Another source of uncertainty is the aerosol variability at scales smaller than the model's grid box, which can hamper the representation of aerosol optical properties. This fact was brought to light in Weigum et al. (2016), where the aerosol water uptake through aerosol-gas equilibrium reactions was established as one of the most affected processes by this variability. The inherent non-linearities in these processes result in large changes in aerosol properties which are exaggerated by convective transport. The uncertainties in RH also contribute to those of aerosol optical properties due to their dependence in hygroscopic growth (Yoon and Kim, 2006; Zhang et al., 2012; Altaratz et al., 2013; Palacios-Peña et al., 2019a).

Bearing in mind the uncertainties described above, the aim of this work is to shed some light on the uncertainties when representing aerosol optical properties. In order to achieve this ~~objective~~aim, this contribution quantifies the sensitivity of aerosol optical properties and their vertical distribution (which may condition aerosol radiative forcing) to several aerosol processes and parameters. ~~The sensitivity tests were~~ This quantification has been estimated by sensitivity tests carried out using the WRF-Chem regional fully-coupled model~~by modifying~~ . Modified aerosol processes and parameters are dry deposition, sub-grid convective transport, relative humidity and wet scavenging.

2 Methodology

Sensitivity tests have been conducted to assess the impact of the most relevant processes for representing aerosol optical properties. For that, the WRF-Chem model (Grell et al., 2005) version 3.9.1.1 has been utilized. The 2010 Russian heatwave/wildfires episode has been selected as a case study because of the literature available referring to this episode (see section 2.1). To achieve this objective, aerosol dry deposition velocity, sub-grid convective transport, aerosol water uptake and wet scavenging were the processes scaled. The degree of impact of these processes is evaluated by analyzing the AOD at 550 nm, different vertical profiles for extinction (α) and backscatter coefficient (β) at 532 nm, and the concentration profiles of different aerosol species. The AOD is defined as the vertical integral of extinction in the total atmospheric column.

2.1 The 2010 Russian wildfires and heatwave episode

The 2010 Russian wildfires and heatwave episode occurred approximately from 25 of July to 15 of August 2010 and lasted a total of 22 days. This was an anomalous heatwave, termed as “mega-heatwave" by Barriopedro et al. (2011), with ~~monthly mean temperatures in the summer months 5–9 °C higher than those for 2002–2009 due to~~ a prolonged blocking anticyclone situation which ~~triggered large~~ favoured an increase of the summer temperature (close to 9 degrees larger than 2002-2009 summers) promoting to larger wildfires (Bondur, 2011). This prolonged blocking situation has been attributed to the global warming leading to very high sea surface temperatures in several places around the world, due to the action of the ENSO (El Niño Southern Oscillation) which altered the atmospheric circulation by forcing quasi-stationary Rossby waves (Sedlàček et al., 2011; Lau and Kim, 2012; Trenberth and Fasullo, 2012). In addition, according to Rahmstorf and Coumou (2011) the 2010 July heat record in Moscow was caused by the climate warming with approximate 80 % probability.

With respect to air quality, this is a well-known and widely studied episode. Many of these works analyzed the physico-chemical characteristics of the smoke from wildfires and the effects on air quality of the transport (both particles and trace gases) to surrounding areas (Zvyagintsev et al., 2011; Witte et al., 2011; van Donkelaar et al., 2011; Gorchakov et al., 2014; Safronov et al., 2015); medium-range transport (e.g. Finland) (Portin et al., 2012; Mielonen et al., 2013) or long-range transport, even reaching Greece (Diapouli et al., 2014).

Among all these reasons, this heatwave has been extensively investigated because of the particularly significant interactions between meteorology and chemistry/particles during this strong air pollution episode (Makar et al., 2015b, a; Kong et al., 2015). This episode was one of the case studies within the COST Action ES1004 EuMetChem (European framework for online integrated air quality and meteorology modelling; see http://www.eumetchem.info/) chosen from the previous experience of Phase 2 of the Air Quality Modelling Evaluation International Initiative (AQMEII; Galmarini et al., 2015).

The effects of air pollution on meteorology where evinced by Konovalov et al. (2011), Chubarova et al. (2012) and Wong et al. (2012) among others. These studies demonstrated changes in atmospheric regional conditions caused by a modification in the composition of atmospheric gases; and also because of changes in optical and radiative characteristics of aerosols coming from the fire emissions. Gorchakov et al. (2014) detected a regional mean AOD of 1.02 ± 0.02 and a ~~very high~~ single-scattering albedo ~~(~~of 0.95~~)~~; and estimated a regional mean aerosol radiative forcing at the top and the bottom of the atmosphere of -61 $\pm$ 1 and -107 $\pm$ 2 W m^{-2}, respectively.

When aerosol interactions were taken into account, a reduction of solar radiation on the ground up to 50 W m^{-2} in diurnal averages and in the near-surface air temperature between 0.2 and 2.6 °K was evaluated on a regional scale over most of eastern Europe. Similarly, a reduction in the planetary boundary layer (PBL) height from 13 to 65 % and the vertical wind speed from 5 to 80 % were found by Péré et al. (2014). Baró et al. (2017) reported similar results on surface winds caused by a decrease of the shortwave downwelling radiation at the surface, leading to a reduction of the 2-m temperature and hence reducing the turbulent flux and developing a more stable PBL. This cooling increases both the surface pressure over the Russian area and the RH (with values around +3.5 %). In the same case, Forkel et al. (2016) manifested a reduction between 10 and 100 W m~~^{2}~~$^{-2}$ in the average downward short-wave radiation at the ground level and a drop in the mean 2-m temperature of almost 1 °K

over the area where the fires took place. On the other hand, Péré et al. (2015) evaluated the impact of aerosol solar extinction on the photochemistry, resulting in a reduction of the photolysis rates of NO_2 and O_3 up to 50 % (daytime average) due to the aerosol extinction along the aerosol plume transported, as well as a reduction of the formation of secondary aerosols.

2.2 Model setup

As aforementioned, the version 3.9.1.1 of the ~~fully coupled~~ fully-coupled on-line WRF-Chem model (Grell et al., 2005) was used in order to simulate transport, mixing, and chemical transformation of trace gases and aerosols coupled to the meteorology (thus including ARI and ACI processes, among others).

Figure 1 displays the target domain of the simulations which covered Europe with a horizontal resolution of $\sim$23 km. However, in order to focus on the aerosol effects, a smaller window covering between 40 and 65 ° N and 20 and 60 ° E (green box in Figure 1) was defined.

The definition of the modelling domain, initial and boundary meteorological and chemical conditions and different emissions has been built on the previous experiences of the COST Action EuMetChem and Phase 2 of the AQMEII initiative. However, in this case the simulations are continuous runs instead of reinitialized every 48 hours (two-day time slices) as done in AQMEII and EuMetChem methodologies (Forkel et al., 2015). A spin-up period of five days has been considered for running the sensitivity tests.

Meteorological initial and boundary conditions (3-hourly data and 0.25° resolution) were provided by the European Centre for Medium-Range Weather Forecasts (ECMWF) operational archive. Chemistry boundary conditions (3-hourly data and 1.125° resolution) for the main trace gases and particulate matter concentrations were taken from the ECMWF Integrated Forecasting System – Model for Ozone and Related Chemical Tracers (IFS-MOZART) model run in the (MACC-II) project (Monitoring Atmospheric Composition and Climate-Interim Implementation; Inness et al., 2013).

Annual anthropogenic emission ($\sim$7 km resolution), whose details are described in Im et al. (2015a, b), came from the Netherlands Organization for Applied Scientific Research (TNO) MACC emissions inventory (http://www.gmes-atmosphere.eu/; Pouliot et al., 2012; Kuenen et al., 2014; Pouliot et al., 2015). CH_4, CO, NH_3, total Non-Methane Volatile Organic Compounds (NMVOCs), NO_x, PM (PM~~1~~0 ~~10~~ and $PM_{2.5}$) and SO_2 were available by 10 activity sectors. Schaap et al. (2005) provided temporal ~~profiles~~ (diurnal, day-of-week, seasonal) and vertical emission profiles. Biomass burning emission data of the total PM emissions (daily data with a spatial resolution of 0.1 °) were derived from the project IS4FIRES (Integrated monitoring and modelling system for wild-land fires; Sofiev et al., 2009). ~~Other biomass burning emission species were estimated after Im et al. (2015b).~~ As described by Soares et al. (2015) emissions were calculated from a re-analysis of the fire radiative power from MODIS on-board of Aqua and Terra satellites and calibration emission factors based on the comparison between observations and modelled data processed by the System for Integrated modeLing of Atmospheric coMposition (SILAM). Day and night vertical injection profiles were also provided. Finally, total PM emissions were transformed to WRF-Chem emission species following Andreae and Merlet (2001) and and Wiedinmyer et al. (2011). No heat release due to the fires was considered. Uncertainties of this biomass burning emissions dataset were estimated by Soares et al. (2015) with an overestimation in-average of 20–30 % which could raise to about 50 % in specific episodes. This impacts on total emissions likely come from

under-stated injection height which can lead to overestimation of the near-surface concentration and reduction of elevated plumes; or a misinterpretation by MODIS of oil and gas flares and large industrial installation as fires. More details can be found in Soares et al. (2015). Table 1 summarizes the physico-chemical parameterizations and schemes used in the simulations.

The skills of the model to represent AOD during this episode have been evaluated in depth in Palacios-Peña et al. (2018) and Palacios-Peña et al. (2019a). The model skillfully represents low and mean AOD values albeit underestimates the high AOD over the Russian area due to two different hypothesis: 1) not considering the fire emissions from small fires (Toll et al., 2015; Wooster et al., 2005) or 2) a misrepresentation of the aerosol vertical profile based on the understated injection height of the total biomass burning emissions found by Soares et al. (2015).

2.3 Sensitivity tests

Table 2 summarizes the sensitivity tests carried out. As previously mentioned, the processes selected to be scaled include RH, dry deposition, sub-grid convective transport and wet scavenging. They were chosen because they are considered as key sources of uncertainty when modelling atmospheric aerosol properties and thus they are expected to impact the estimation of aerosol optical properties (e.g. Ackermann et al. (1998); Lee et al. (2013); Quan et al. (2016), among many others).

RH highly impacts aerosol properties by affecting several processes such as nucleation, chemistry or uptake of water through aerosol-gas equilibrium reactions (Ackermann et al., 1998). Because of that, our sensitivity test for this variable modified the RH in the aerosol module of WRF-Chem (precisely, in the part of the code when RH enters the aerosol module). Henceforth, RH modification only affects aerosol properties and not meteorology. Following the evaluation of this meteorological variable conducted by Tuccella et al. (2012) and Žabkar et al. (2015), it was scaled to 0.9 (a reduction of 10 %). Although the translation into saturation only applies at saturation conditions, supersaturation values higher than 1 % are unlikely. Because of that, this variable could not be scaled by +10% (to 1.1), and hence the chosen upper values were 1.005 and 1.01; that is, 0.5 % and 1 % supersaturation respectively.

In this work, dry deposition velocity (DDV) is estimated by the MADE module (Ackermann et al., 1998) as in the Regional Particulate Model (RPM; Binkowski and Shankar, 1995). But in contrast to RPM, MADE calculates and applies deposition velocities separately for each mode (Aitken, accumulation and coarse). The method uses the aerodynamic resistance, the settling velocity and Brownian diffusivity; and then, the Slinn and Slinn (1980)'s and Pleim et al. (1984)'s expressions are calculated by averaging the quantities over the k^{th} moment of the distribution as in Kramm et al. (1992). The modification for our sensitivity test regarding dry deposition consists on scaled DDV by the values indicated in Table 2. Following Lee et al. (2013), DDV has been scaled to 0.5 and 2 for the Aitken mode and 0.1 and 10 for the Accumulation mode, which are the both ends of the uncertainty range of these parameters. WRF-Chem configuration gives the opportunity to turn on/off the dry deposition of gases and aerosols. Thus, another sensitivity case corresponds to the WRF-Chem configuration with the dry deposition of aerosol turned off (aer_drydep_opt = 0 in the namelist of the model).

Analogously to dry deposition, sub-grid convective transport in WRF-Chem can be turned on/off. This process is parametrized by a simple scheme (Grell and Dévényi, 2002) based on a convective parametrization developed by Grell (1993) and Grell et al. (1994). This scheme estimates the output temporal tendency (s^{-1}) separately in the bottom layer and the rest of the layers.

Afterwards this tendency is applied to the chemical concentration for each species in order to estimate the sub-grid convective transport. This tendency has been modified in our sensitivity test as indicated in Table 2. Following the evaluations carried out by Doherty et al. (2005) and Quan et al. (2016), the output temporal tendency has been scaled to $\pm 50\,\%$. Moreover, a case with sub-grid convective transport turned off (chem_conv_tr = 0 in the model's namelist) has been run.

Aerosol wet scavenging in WRF-Chem follows the approach of Easter et al. (2004). This process is produced by impacting/interception and precipitation, when all aerosol species are assumed to be immediately wet-deposited. The model distinguishes between wet scavenging for large-scale and sub-grid stratiform and sub-grid convective clouds. Both, stratiform (wetscav_onoff) and convective (conv_tr_wetscav) wet scavenging can be turned on/off in WRF-Chem. A case in which stratiform wet scavenging is turned off was run. This modification has been chosen because the evaluated episode was an anticyclonic situation without important convective clouds.

3 Results and discussion

In this section the results of the sensitivity of AOD representation to changes in RH, DDV, wet scavenging and convective transport are assessed, focusing on the Russian region affected by the heatwave-wildfire episode. Afterwards, a local evaluation of the vertical profiles is carried out in order to establish the influence of each process on aerosol vertical profiles.

3.1 Changes in total AOD

Figure 2,~~top~~ top-right displays the modelled AOD at 550 nm for the base case. The rest of the Figure 2 depicts the differences between the sensitivity experiments and the base case. ~~The top-right figure shows the mean bias.~~ For the base case, high AOD values (up 0.5) are found over a large area of central Russia, including populated cities such as Moscow, Nizhny Novgorod or Kazan. AOD values around 0.3, are found over a wider area close to the Finnish border (northwest of the domain) and over most of Belarus, Ukraine and the Black Sea (south of the domain). The lowest values (around 0.1) are found over central Europe. The changes of AOD in the sensitivity experiments are shown in the other pannels of Figure 2

Figure 2,*a*, *b* and *c* represent the sensitivity to RH: a decrease of 10% (L10RH); an increase of 0.5% (H05RH); and an increase of 1% (H1RH), respectively. As expected, a 10% decrease of the RH leads to a stronger response compared with the experiments when RH increases since the percentage of modification is lower in the latter sensitivity tests. L10RH (Figure 2,*a*) experiment shows positive differences at the west of the Volga river, reaching values around +0.6. Oppositely, there are negative differences of -0.15 in the area placed eastern to the Volga. Meanwhile, the H05RH (Figure 2,*b*) experiment shows this positive (west)/negative (east) dipole over the fire-affected area but differences are lower than 0.15.The H1RH experiment (Figure 2,*c*) promotes an increase of AOD encompassing most of the fire-affected area with values around +0.2.

Figure 2,*d* stands for the No-Dry Deposition case (NO_DD): Figure 2,*e* and *f* are the experiments with Low and High Dry Deposition for the Aitken mode, respectively (LDDV_AIT and HDDV_AIT); and Figure 2,*g* and *h* represent the tests modifying the Accumulation mode (LDDV_ACC and HDDV_ACC). All the experiments related to changes in dry deposition (Figure 2,*d*-*h*) showed ~~the~~ its strongest response located over the wildfires area, but ~~less significant~~this response is less relevant

than for other cases. Figures 2,*d*, NO_DD, and *e*, LDDV_AIT, have a similar spatial pattern of differences with positive changes (up to +0.35 and +0.2, respectively) at the western Volga river. However, increasing the dry deposition in Aitken mode (Figure 2,*f*) and both increasing and decreasing the deposition in accumulation mode (Figures 2,*g* and *h*) ~~provokes~~ provoke negative changes of AOD over the eastern Volga (around -0.3 in all of these cases). HDDV_ACC is the only test which produces a general reduction in AOD over most of the study area (temporal and spatial mean change in AOD of -0.06) but this differences are stronger over fire affected areas and downwind.

Figure 2,*i* shows the No sub-grid Convective Transport (NO_CONV_TR) case and Figure 2,~~*j*~~*k* the High sub-grid Convective Transport (HCONV_TR) case. Both of them evidence negative differences (up to -0.39 and -0.43, respectively) over the fire-affected and downwind areas. However, the NO_CONV_TR case displays stronger positive differences over the northeastern part of the domain (up to +0.25) which do not occur for the HCONV_TR experiment. Figure 2,~~*k*~~*j* indicates that the Low sub-grid Convective Transport case (LCONV_TR) ~~presents smooth differences~~ has lower absolute differences are lower. A dipole of positive and negative differences (which means higher and lower AOD than the base case) is found over all the domain, a bit stronger over the fire-affected area.

Finally, turning off the scavenging (Figure 2,*l*; NO_WS experiment) leads to positive differences over a large part of the area with values higher than +0.2 over the north and west zones of the target domain. Moreover, temporal and spatial mean AOD difference (0.04) is the second largest even though there are not many clouds in the studied domain (see Figure 3 in Supplementary Material). This implies that wet scavenging could be really important when there are clouds present.

3.2 Optical properties and concentration profiles of different species: disentangling the causes of AOD changes

In order to disentangle the cause of the differences in the sensitivity tests, this section discusses the temporal mean of the vertical profiles of optical properties and concentration of several chemical species over specific locations of the target area. Figure 2, top-left displays ~~where~~ the spot where the vertical profiles are estimated. The choice of these locations claims to bring light to the behaviour aloft over different places in the target area. Because of that, the locations where the ~~time~~ temporal mean of AOD was minimum and maximum, respectively, were selected and named as Min-AOD and Max-AOD. A profile over Moscow, one of the most fire-affected cities, was also chosen to evaluate the fire plume effect downwind.

In addition to α, β and lidar ratio (LR), concentrations for different species were evaluated: elemental carbon (EC), primary organic aerosol (POA), secondary organic aerosol (SOA), sea salt (SEA), nitrate (NO_3^-), ammonia (NH_4^-) and sulphate (SO_4^{2-}).

Vertical profiles over the Max-AOD location are shown in Figure 3. α and β ~~present similar profiles~~have similar shapes. The base case shows a profile with high values (above 0.6 km^{-1} for α and below 0.02 $km^{-1}sr^{-1}$ for β) at the surface. Both values decrease with height until around 0.2 km^{-1} for α and 0.005 $km^{-1}sr^{-1}$ for β at 900 hPa. Afterwards, values increase again to 0.3 km^{-1} for α and 0.01 $km^{-1}sr^{-1}$ for β at around 800 hPa (indicating the presence of aerosols associated to fire emissions aloft), where hereinafter decrease. Values are close to 0 above 600 hPa.

LR represents the ratio of the extinction and the backscatter coefficients and is usually used to characterize the type of particles. This variable ranges from 1 to 100 sr~~$^{-1}$~~ $^{-1}$ (Fernald et al., 1972). Following this definition, low LR values are expected for large and scattering particles and high LRs are expected for absorbing particles. Typical LRs at 532 nm are

20-35 sr~~−1~~ $^{-1}$ for sea salt, 40-70 sr~~−1~~ $^{-1}$ for desert dust, 70-100 sr~~−1~~ $^{-1}$ for biomass burning aerosols and 45-75 sr-1 for urban/continental aerosols (Müller et al., 2007). The vertical profile of LR displays low values of around 35 sr^{-1} at low heights. LR increases to values between 50 and 60 sr^{-1} around 700 hPa. Higher up, between 500 and 300 hPa, LR reaches values around 65 sr^{-1} which again, above 300 hPa, decrease to 35 sr $^{-1}$. ~~A remarkable issue is~~ It is noticeable that LR values ~~are~~ over the MIN-AOD location (close to 30 sr $^{-1}$) are not comparable to those values expected by the scientific literature (e.g Mielonen et al., 2013). However, it should be born in mind that MIN-AOD location is affected principally by sea salt, while the aforementioned reference covers a biomass-burning affected area. Moreover, extinction and backscatter modelling profiles shape are similar (rather constant at levels close to the surface~~, contradicting the LR expected from observations.~~), which is not found in most of the observed LR profiles. This could be ascribed to a model misrepresentation of extinction and backscatter modelling profiles. For example, Mielonen et al. (2013) measured the LR during the same forest-fire event in Finland. These authors found LR values of 60-70 sr^{-1} for layers below 2 km, pointing to a mixture of biomass burning aerosols and other less absorbing aerosols. Conversely, in the upper layers the LRs were around 55 sr~~−1~~ $^{-1}$, which indicated the presence of polluted dust. This reveals the misrepresentation in the LRs by our simulations, which estimate LRs around 35 sr-1 (typical LR values for sea salt particles) over areas with a high concentration of biomass burning aerosols (LR should typically reach values higher than 60 sr~~−1~~ $^{-1}$).

In order to assess which species has the strongest influence on α and β, and also which chemical species presents the highest sensitivity in the designed experiments, profiles for the different species are shown in Figure 3, 5 and 7. Overall, total concentration is highly determined by the dry concentration, as expected for a heatwave episode. In addition, ~~Figure~~Figures 4, 6 and 8 quantify the mean absolute error (MAE) of each experiment with respect to the base case, and in colors, the normalized MAE (NMAE). ~~This latter statistical figure has been defined by normalizing the mean absolute error with respect to the values in the base case in order to show the magnitude of the relative changes in each sensitivity test for each variable evaluated~~MAE has been estimated by averaging the absolute error of each experiment regarding the base case at each model level. NMAE is the absolute error divided by the base case at each level and then averaged along the column. The NMAE analysis illustrates the relative change of each magnitude and helps to the intercomparison between the sensitivity test.

3.2.1 Sensitivity to the relative humidity

When the sensitivity tests are evaluated over the MAX-AOD location, the experiments changing the RH present a singular response. When RH increases (H05RH and H1RH), the profile of optical properties also increases, as well as the AOD. MAE for the profiles (Figure 4) of α (β) are 0.0101 (0.0005) and 0.0159 (0.0004), for the case in which RH is scaled to 0.5 % (H05RH) and 1 % (H1RH) respectively, and NMAE are 0.4 (0.4) and 0.6 (0.5). These differences could be caused by the high dependence of AOD on water uptake, which finally depends on RH, as indicated by Ginoux et al. (2006); Yoon and Kim (2006); Altaratz et al. (2013); Palacios-Peña et al. (2017, 2018, 2019a). Thus, an increase in RH affects the hygroscopic growth, resulting in larger particles. For this reason, a reduction of optical properties is expected when RH decreases (L10RH experiment). However, the results indicate an increase in AOD and ~~optical properties profiles~~ profiles of extinction and backscatter coefficients

(MAE 0.0162 and NMAE 0.6 for α; and 0.0005 and 0.7 for β). This response is the result of an increase of NO_3^- (MAE 0.8209 and NMAE 0.6) and, in particular, of SOA (MAE 0.2054 and NMAE 0.9).

The concentrations of inorganic species are controlled by the so-called sulphate-ammonium-nitrate-water equilibrium (Seinfeld and Pandis, 2006). NO_3^- and NH_4^- present a deliquescence RH of approximately 60 % (Saxena et al., 1986). However, SO_4^{2-} absorbs water at nearly all RH. As exposed by Weigum et al. (2016), due to the RH absorption by the SO_4^{2-}, the equilibrium is dominated by the reaction in which ammonia neutralizes sulphuric acid and drives the equilibrium towards the aerosol phase ($(NH_4)_2SO_4$). Therefore, ammonia can neutralize nitrate resulting in aerosol phase (NH_4NO_3) only when the total amount of sulphate has been neutralized (i.e. in areas with high concentrations of ammonia and/or low concentrations of sulphate). At this point, sulphate concentrations remain constant, and nitrate increases with aerosol water content.

This sulphate-ammonium-nitrate-water equilibrium explains the behaviour of the inorganic species. For the highest RH case (H1RH), NO_3^- concentration shows a considerable increase while SO_4^{2-} slightly increases. This could be influenced by an increase of the RH favouring the NO_3^- formation together with a high sulphate concentration for which most of the sulphate has been neutralized.

However, in the case with a reduction of the RH in a 10 % (L10RH), NO_3^- displays a similar concentration as the base case at surface levels and ~~higher at levels above~~ around 800 hPa. Throughout the rest of the profile concentration is higher than in the base case but not as higher as in the H1RH case. Meanwhile, SO_4^{2-} concentrations are much higher than for the base case. Sulphate concentrations are favoured by its low deliquescence point which promotes its formation. In spite of that, at higher levels, sulphate concentrations were at the point in which most of the sulphate has been neutralized favouring NO_3^- formation, producing higher NO_3^- concentrations in the L10RH case.

The H05RH (RH scaled to 1.005) experiment shows optical properties and concentration profiles closer to the base case, which can be caused by the low RH modification, so that inorganic species are not highly affected by this change.

Changes in the profiles of inorganic species do not clarify the results found for the modifications in the profiles of optical properties (and AOD). These modifications are led by changes in SOA. In both H1RH (RH scaled to 1.1) and L10RH (RH scaled to 0.9), SOA profiles depict an increase in their concentrations resulting in an increase of α and hence AOD. Moreover, this increase is higher for the L10RH case. This positive variation in SOA profiles are explained by the use of the VBS mechanism (Ahmadov et al., 2012). As pointed out by Tuccella et al. (2015), in this mechanism volatile organic compounds(VOC) are oxidized by reactions with the ~~hidroxy~~ hydroxyl radical (OH), O_3, and nitrate radical (NO_3^-, producing organic mass in two different regimes of high and low NO_x). In the former, organic peroxy radicals react with nitrogen monoxide (NO); conversely, in the latter organic peroxy radicals react with other organic peroxy radicals. The organic matter produced is partitioned into aerosol and gas phase assuming a pseudo-ideal partition.

Thus, SOA profiles for the RH case depict two different types of behaviour: (1) Above 950 hPa (around the PBL height, see Figure 1 in the Supplementary Material~~,~~) the shape of the NO_x and SOA profiles are similar, and thus, at these vertical levels, variations in SOA concentrations may be due to ~~the effect described by Sarrafzadeh et al. (2016):~~ an increase in NO_x concentrations at low-NO_x conditions ~~(less than 30 ppb or around 55 μg m^{-3})~~(less than 30 ppb or around 55 μg m^{-3}; Sarrafzadeh et al., 2016) ; (2) Below 950 hPa the RH effect is added to the effect of NO_x described above in (1). Therefore, in the H1RH case, SOA are

higher because the concentration of this species increases due to NO_x oxidation and RH, meanwhile in the L10RH case the positive variation of the concentration of SOA caused by the RH is limited. That means that this variation depends more of RH modifications (see Figure 2 in the Supplementary Material) than NO_x oxidation.

Over the MIN-AOD, the RH scaled to 0.9 (L10RH; NMAE $>$ 0.6 except for SEA, 0.1) should be highlighted. Despite L10RH does not ~~provokes~~ provoke a strong difference in AOD, changes in organic species are relatively strong and are similar to those changes in β profile. A reduction of RH may favour the increase of the concentration of these species. α profile is similar to NO_3^-. In this case, these changes could be due to the actions of the nitrate-ammonia-sulphate equilibrium.

Finally, to elucidate the response of the different experiments over a downwind location, profiles over Moscow are shown in Figure 7. The response for most of the experiments is similar as over the MAX-AOD location; but in this case L10RH (RH scaled to 0.9) experiment shows a stronger response (NMAE $>$ 1.5 for most of the variables) due to higher NO_3^- concentrations. Over this location RH is higher than over the MAX-AOD, favouring the formation of NO_3^-. POA displays higher concentrations for the L10RH case, likely due to a competition of SOA formation between NO_3^- and POA.

3.2.2 Sensitivity to dry deposition

Regarding dry deposition over the MAX-AOD location, the no dry deposition case (NO_DD) shows an increase in the AOD over the target area and displays higher α and β values than for the base case at near-surface levels. However, above 950 hPa (around the PBL height, see Figure 1 in the Supplementary Material), the optical profiles decrease to levels lower than those for the base case. Despite this decrease aloft, total AOD increases (Figure 2) likely because the highest concentrations for chemical species are located at these levels. With respect to the different species, all of them present higher concentrations than the base case, in particular at levels below 950 hPa. MAE (NMAE) of α and β for this experiment are 0.0283 (1.1) and 0.0008 (1.1, Figure 4).

Changes in dry deposition experiments occur in those modes where modifications were implemented (Figure 4 in the Supplementary Material). When modifying the deposition of the accumulation mode, the Aiken mode does not present important changes and thus the observed variations come from the accumulation mode. However, when modifications are implemented in the deposition of the Aitken mode, both modes are affected, since particles in the Aitken mode quickly experience coagulation processes and turn into particles in the accumulation mode.

A higher AOD is also found for the LDDV_AIT case (low dry deposition velocity in the Aitken mode). For this experiment, α (MAE 0.0205 and NMAE 0.8) and β (MAE 0.0005 and NMAE 0.7) exhibit higher values at the surface (around 1000 hPa) and between 900 and above 600 hPa. With respect to the profile of the different species, those emitted directly into the atmosphere (primary species) present higher concentrations than the base case at surface levels (around 1000 hPa and below 800 hPa, respectively). This is observed for POA (MAE 2.1988 and NMAE 0.7) and SEA (MAE 0.0154 and NMAE 0.4). However, ~~those species~~ secondary aerosol; which are not directly emitted ~~but~~ and are products of atmospheric chemistry~~(secondary aerosols),~~ ; such as SOA (NMAE $>$ 0.8 and MAE 0.2283) and most of the secondary inorganic species have their concentrations peak ~~higher~~ at a higher altitude than those in the base case between 900 and 600 hPa. These two facts explain the response of the profiles for the optical properties.

As expected, both high DDV experiments (HDDV_AIT and HDDV_ACC, in the Aitken and the accumulation mode respectively) exhibit a reduction of AOD, in particular over the ~~fires~~ fire area. The response of the ~~optical properties profiles~~ profiles of optical properties is similar for both cases and for most of the species. For example, MAE (NMAE) are 0.0365 (0.8) and 0.0392 (1.5) for α. Only SEA shows a different behaviour between the increase of DDV for Aitken (NMAE 0.7) or accumulation mode (NMAE 0.8). The reduction of the total concentration of SEA is higher when DDV is modified in the accumulation mode. This is produced because this species presents most of its concentrations in the Greenfield gap (particle radii of the range of 0.1–1 μm where Brownian motion is not large anymore and gravitational settling is not yet important; Green , the accumulation and the coarse mode and not in Aitken. Regarding organic species (EC, POA and SOA), concentrations are a bit lower when the DDV is modified in the accumulation mode, probably because most of the mass of these species is in this mode (NMAE around 1.4 for all of them). This response is similar to those experiments for SO_4^{2-}, but it is the contrary for NO_3^- because of the the action of the nitrate-sulphate-ammonium equilibrium.

The low dry deposition velocity in the accumulation mode (LDDV_ACC) experiment does not show the *a priori* expected response. AOD decreases over the fires; also optical properties profiles displays lower values: MAE (NMAE) 0.0331(1.3) for α and 0.001(1.3) for β. When the profiles are analyzed, the response differs between species. EC, POA and NO_3^- shows a slight reduction in their concentration, and SOA exhibits a large reduction. Conversely, SO_4^{2-} and SEA display higher concentrations, in particular, at near-surface levels. The response of these latter is the expected when DDV is decreased in the accumulation mode but, despite this increase, the decrease of AOD is the result of the large reduction of SOA concentrations (NMAE 1.1). These SOA reductions may occur due to the increase in SO_4^{2-} concentrations (NMAE 1). By modifying the DDV, SO_4^{2-} concentrations increase, then the nitrate-sulphate-ammonium equilibrium results in a reduction of NO_3^-, which influences SOA formation (as explained above) by decreasing their concentration.

Due to the different behaviour over the MIN-AOD location with respect to those areas affected by wildfires, the no dry deposition (NO_DD; NMAE > 0.9 for all the variables) should be highlighted. For NO_DD, β profile is similar to the profiles of organic species (EC, POA and SOA) as well as NH^{-4} and S_4^{-2} while α is similar to NO_3^-. Organic species present a higher concentration when dry deposition is turned off, resulting in an increase of β. However, NO_3^- decreases, probably due to its competition with SO_4^{2-} (which increases), leading to a decrease close to the surface of α. However, these changes in optical properties profiles are not highly represented by a strong modification of total AOD.

Over the Moscow location, the NO_DD experiment also displays a strong response (NMAE > 1 for all the variables). This response is explained by an increase in the concentration of all the species, in particular, at the surface due to the effect of turning off dry deposition resulting in an increase of α and β.

3.2.3 Sensitivity to sub-grid convective transport

When sub-grid convection is modified, in both experiments NO_CONV_TR (convective transport turned off) and HCONV_TR (scaled ~~to~~ by 1.5) there is an AOD reduction over the fire area. This decrease is also reflected in optical properties over the MAX-AOD location and for most of the species (NMAE > 0.8 in both experiments) except SO_4^{2-}. For ~~these species,~~ POA, EC and SO_4^{2-}, the NO_CONV_TR experiment exhibits a concentration profile similar to the base case with slightly

higher concentrations at surface levels and lower at higher levels (NMAE 0.4). The opposite behaviour is displayed by SEA concentrations. Moreover, SOA, NO^{-3} and NH^{-4} concentration are constantly smaller than the base case. However, the SO_4^{2-} concentration profile for the HCONV_TR experiment shows lower concentrations (NMAE 1.2). Both responses could be caused by modifications in sub-grid convective transport. When this transport is turned off there is a decrease in the particle mixing in the atmosphere and small differences with the base case are found. However, when this transport is increased, involving an increase in all-direction convective transport and not only updraft convection, there is a higher mixing of particles. This fact can favour the transport to levels closer to the surface and then enhance the deposition processes.

For the HCONV_TR experiment, the behaviour of SO_4^{2-} is similar to the rest of the species. Thus, the modification in sub-grid convective transport controls the response of this experiment. However, for the NO_CONV_TR test, the rest of the species behave differently ~~as~~ than SO_4^{2-}. NO_3^- strongly decreases due to the effect of the nitrate-ammonium-sulphate equilibrium in which the sulphate is an obstacle for NO_3^- formation. This low NO_3^- concentration results in a decrease of the SOA formation and consequently its concentration. This finally leads to a decrease of α and AOD. The response of LCONV_TR (convective transport scaled to 0.5) shows a transition between the two extreme cases (NMAE around 1 for all of the variables except SEA, 0.1, and SO_4^{2-}, 0.4).

Over the MIN-AOD location, the behaviour observed for the LCONV_TR experiment (convective transport scaled to 0.5) is also noteworthy albeit NMAE does not have a strong response. AOD is not strongly modified but the profiles of optical properties ~~show a peak in their profiles~~ how a peak around the PBL height. This peak is due to an increase in the concentrations of EC, POA, SOA and NO_3^-. For the organic species, this increase can be due to the modification in the sub-grid convective transport. The presence of these species at this level seems to favour the formation of NO_3^- instead of SO_4^{2-}.

3.2.4 Sensitivity to wet scavenging

The modification of wet scavenging over the MAX-AOD location displays a slight reduction of AOD, which is the result of lower α and reduced concentration of species above the PBL (at 950 hPa). NMAE is < 0.8 for most of the studied variables. This reduction is observed despite the inorganic species (SEA, NO_3^-,NH_4^- and SO_4^{2-}) show higher concentrations at ~~surface~~ the lowest levels. SOA also displays a higher concentration below ~~the PBL~~ 800 hPa but with smaller changes than for inorganic species. This highlights the high impact of organic species on optical properties. All the observed changes can be attributed to changes in the aqueous phase reactions because over these locations stratiform clouds were not present.

To conduct the analysis where clouds were formed during the 2010 wildfires episode (see Figure 3 in the Supplementary Material), the MIN-AOD location is shown in Figure 5. Over this location, the NO_WS experiment ~~is that with~~ has the strongest response regarding optical properties profiles and concentrations for different species. NMAE is above 1.5 for all the studied variables. The profiles of optical properties depict much higher values than for the base case, which are also observed in all of the species. This could be due to the fact that over this area stratiform clouds were present, so the effect of wet scavenging is important over this location.

It should also be highlighted~~that over the MIN-AOD and Moscow spots,~~ , the profile shape of EC and POA ~~profiles of the assessed experiments~~ over the MIN-AOD and Moscow show larger differences ~~between them~~ than over the MAX-AOD

~~. This fact could be explained because over these locations these~~ area for the different experiments. These differences in the shape profiles could be attributed to these species are not ~~being directly emitted~~ directly emitted over MIN-AOD and Moscow areas and transport processes could be influenced by vertical distribution. Moreover, the farther the location is, the ~~larger the differences are.~~ more different the shape of the vertical profile is.

4 Discussion

The main finding of this work is the non-linear response exhibited by AOD to the sensitivity of different key processes. This response is highly dependent on the thermodynamics equilibrium sulphate-nitrate-SOA, in which also water and ammonia operate. Moreover, and probably due to the nature of this episode, SOA shows a high impact on aerosol optical properties representation which was also found by Regayre et al. (2018) and Yoshioka et al. (2019). These works highlighted a large uncertainty in effective radiative forcing due to ARI because of carbonaceous aerosols in high-emission months and in regions close to emission sources. However, under other conditions, the global influence of anthropogenic sulphate aerosol (not only due to emission ; and in lesser extended nitrate (Balzarini et al., 2015); presented a significant influence on AOD estimations. Thus, a large effort should be devoted to the process understanding of this non-linear response from different key sources (RH, convective transport, dry deposition and likely other aerosol processes) and the improvement of representation of the sulphate-nitrate-ammonia-water equilibrium in models for a reduction in aerosol uncertainty. From a global point of view, different works found the processes evaluated in this work to be important sources of uncertainty when characterizing aerosol optical properties and/ or radiative forcing (which is highly influenced by the latter). Regayre et al. (2018) found the deposition rate of aerosols and aerosol precursors (gases) to be the most important causes of the uncertainty related to effective radiative forcing. Also, dry deposition was the most important process for global mean CCN uncertainty (Lee et al., 2013), a source of uncertainty in AOD representation (Romakkaniemi et al., 2012). Although this process presents large uncertainties in AOD estimation in the aforementioned work, its importance is limited over a fire-affected region. Thus, attention should be taken in the evaluation of the uncertainty of this process depending on the scale, since likely the impacts of this process would be stronger over other regions, making it important globally. As was pointed out by Regayre et al. (2018) some uncertainty causes in radiative forcing could be because they cause at least a small amount of uncertainty in nearly all regions or because they are the largest causes in some regions. Both Lee et al. (2013) and Regayre et al. (2018) used global models (GLOMAP-mode within the TOMCAT global 3-D offline chemistry transport model and HadGEM-UKCA model, respectively) during a whole year. Moreover, it should be highlighted that CCN uncertainty affects not only AOD representation but also to radiative forcing uncertainties due to ACI (Lee et al., 2013).

Similar results were found by Kipling et al. (2016) but for convective transport using the HadGEM3-UKCA model. This process was found to be very important in controlling the vertical profile of all aerosol components by mass. In addition, previous works as Palacios-Peña et al. (2018) and Palacios-Peña et al. (2019a) found that a misrepresentation of aerosol vertical profile could lead to uncertainties in the representation of AOD. On the other hand, Croft et al. (2012) evaluated the uncertainty due to different assumptions for the wet scavenging of aerosol and found a 20 to 35 % uncertainty in simulated global, annual

mean AOD using the ECAM5-HAM model. However, the findings in our work regarding wet scavenging were lower due to the type of episode selected (without extensive clouds).

Another source of uncertainty is that related with general circulation. In this sense, Nordling et al. (2019) demonstrated a significant uncertainty in regional climate responses due to differences in circulation even with perfect aerosol descriptions. In addition, Brunner et al. (2015) pointed out the need for improving the simulations of meteorological parameters relevant for air quality. On the other hand, other works found an effect on meteorological variables, and thus, in circulation responses when aerosol effects are taken into account. This source of error is more relevant during the summer and near large sources of pollution (Makar et al., 2015b; Baró et al., 2017), conditions that are similar to the episode analyzed here. These works show an impact on shortwave downwelling radiation at the surface, temperature, RH and PBL height due to the inclusion of aerosol effects which again could affect AOD uncertainties. Moreover, Kong et al. (2015) evidenced an improvement in the skill of meteorological variables when aerosol radiation effects were included. Thus, the uncertainties in the representation of the vertical distribution of aerosols and their optical properties revealed in this work could be limited to the influence of the regional circulation response, which in turn could again impact the aerosol distribution. Because of that, a reduction in this aerosol uncertainty could reduce the uncertainty in circulation response and thus, the evaluation of uncertainty could be constrained only to uncertainties in circulations mechanisms, as pointed out by Nordling et al. (2019).

Other important sources of uncertainty in aerosol optical properties representation among those evaluated here are the aerosol emissions (Granier et al., 2011; Soares et al., 2015), representations of complex sub-grid processes (Weigum et al., 2016), aerosol processes (Croft et al., 2012), subsequent feedbacks on atmospheric dynamics (Booth et al., 2012; Bollasina et al., 2013; Villarini and Vecc , aerosol mixing (Zhang et al., 2012; Curci et al., 2019) and aerosol size distribution (Tegen and Lacis, 1996; Claquin et al., 1998; Eck et al . Another source of uncertainty is the choice of the aerosol-chemical mechanisms which was pointed out by Balzarini et al. (2015) and Palacios-Peña et al. (2018, 2019a).

In order to simplify the approach this study has been conducted using only one model; however, differences among models and how these represent the life cycle of aerosols should be kept in mind (Randles et al., 2013; Kim et al., 2014; Mann et al., 2014; Tsigarid and similar studies with other model approach are necessary for an overall knowledge of these uncertainties.

5 Summary and Conclusions

Aerosol optical properties (e.g. AOD) are highly influenced by the vertical distribution of atmospheric aerosols, which also condition the representation of ARI and ACI processes and their uncertainty. Thus, a key issue in climate modelling is the assessment of the uncertainty in the representation of aerosol optical properties. ~~In order to reduce (or, at least, quantify) this uncertainty, this~~ This work assesses the sensitivity of aerosol optical properties and the aerosol vertical distribution to key physical processes. To achieve this objective, sensitivity runs modifying RH, dry deposition, sub-grid convective transport and wet scavenging have been carried out ~~during~~ for the 2010 Russian heatwave/wildfires episode with the WRF-Chem regional ~~fully-coupled model.~~ fully coupled model. Findings in this work would help to improve modelling aerosol representation giving some initial guidelines about what parameters could be misrepresented or are the most sensitive to the vertical mixing.

Results indicate that there is a non-linear response of AOD to different key processes. For example, both an increase and a decrease in the RH results in higher AOD values. A similar non-linear response is found when reducing the dry deposition velocity; in particular, for the accumulation mode, where the concentration of several species increases (a decrease might be *a priori* expected). Also the modifications in the sub-grid convective transport exhibit a non-linear response because both the increase and offset of this process leads to a reduction in the AOD over the fire area. Similar non-linear responses were previously found, among others, by Lee et al. (2013); Kipling et al. (2016) using both different models and experiments; and by Weigum et al. (2016) using the WRF-Chem model as in this work.

With respect to the quantification of the sensitivity, changes in RH of 0.9 lead to the highest AOD differences (0.6). This high sensitivity is followed in relevance by vertical convective transport (with AOD differences around -0.4) and dry deposition (AOD differences up to -0.35 and 0.3). ~~Similar results were previously found, among others, by Lee et al. (2013); Kipling et al. (2016) using both different models and experiments; and by Weigum et al. (2016) using the WRF-Chem model as in this work.~~

However, when RH increases (1.005 or 1.01 scaling factors), the response is weaker (AOD differences lower than 0.15) than when RH decreases. This is because the scaling to high RH values is smaller since an important supersaturation (above 1-2 %; Devenish et a is not realistic in climate models. When the RH slightly increases the AOD changes are conditioned by the water uptake by particles and hence modifying the size of particles by hygroscopic growth (see H05RH experiment). In this case, no large changes in concentrations are found. Nevertheless, for larger modifications (H1RH), changes in AOD are dominated by changes in nitrate and SOA. These changes in SOA are controlled by two mechanisms of particles formation. (1) The first mechanism, the nitrate-ammonia-sulphate equilibrium, explains the changes found for SO_4^{2-} and NO_3^-. Summarizing, the amount of sulphate domains this equilibrium in which ammonia can neutralize nitrate only when there is a high concentration of ammonia and/or low concentrations of sulphate. By this way, if most of the SO_4^{2-} concentration has been neutralized, an increase in RH favours NO_3^- formation. Moreover, in low RH conditions, NO_3^- formation is possible only under low SO_4^{2-} concentrations. (2) The second mechanism which controls SOA formation is the implemented VBS mechanism (Ahmadov et al., 2012; Tuccella et al., 2015). In our experiments, VOC are oxidized by reactions with nitrate radical in the regime of low NO_x and SOA increases as NO_3^- concentrations, as described by Sarrafzadeh et al. (2016).

Dry deposition presents a higher impact for the accumulation mode (NMAE higher than 1.4) than for the Aitken mode (NMAE around 1.3) because a higher mass of fire particles are emitted into this mode. Over the MAX-AOD location switching off the dry deposition does not have a strong impact on AOD, but it does over the rest of the domain. Over this location, particles are directly emitted into the atmosphere while over other locations transport governs the concentrations. In general, when dry deposition is suppressed or reduced, AOD increases and conversely when it is increased, AOD decreases. However, the response over the MAX-AOD location of the decrease of dry deposition for the accumulation mode is noticeable because a decrease in the dry deposition in this mode significantly increases SO_4^{2-} concentrations. Thus, the nitrate-ammonia-sulphate equilibrium reduces NO_3^- leading to a reduction of SOA and then AOD.

The suppression and the increase of the vertical convective transport also presents an impact on the aerosol vertical distribution. When the vertical convective transport is increased all the species show a similar response. This modification implies an increase of the transport not only upwards but also in all directions, increasing the mixing of particles which can favour

the transport from upper layers to the surface, hence enhancing deposition. However, when the sub-grid convective transport is suppressed the nitrate-ammonia-sulphate equilibrium and the SOA formation mechanisms play an important role. A reduction in the vertical convective transport, which can reduce the mixing of particles, results in significant changes of AOD but over regions away from the sources (main emission areas), in particular, over the MIN-AOD spot.

Wet scavenging does not significantly impact the vertical aerosol mass due to the type of episode selected as case study (heatwave with clear skies). There is an impact over the MIN-AOD location because this is a cloudy area during the period of the episode.

Regarding the LR, simulated values of this variable are remarkably different from those observed in the scientific literature, mainly over fire affected areas. In those areas where high LR are expected due to the presence of biomass burning particles, simulations estimate lower LR and viceversa. It should be also pointed out that most of the species show relatively larger differences when they are considered far away from the emissions areas. Thus, as pointed out by Lee et al. (2013), the uncertainty in aerosol microphysical processes becomes increasingly important in remote regions (far from the source of emissions).

To summarize, the sulphate-nitrate-SOA formation is the process with the largest sensitivity and hence the process whose uncertainty can have a larger impact on AOD representation. Changes in this process could come from modifications in RH, dry deposition or vertical convective transport. By itself, dry deposition also presents a high sensitivity which influences AOD representation.

Last, it should be noticed that the processes evaluated here are not the only processes that might condition the uncertainty in aerosol properties. The selection of these experiments has been based on their relevance according to the available literature and their experimental design has been constrained by the high computational cost of these on-line coupled chemistry-meteorological simulations. In this sense, further studies addressing the reduction of the demonstrated uncertainties are needed. Reducing uncertainties of AOD and aerosol representation implies the reduction of uncertainties in the representation of aerosol effects, both ARI (by AOD) and ACI (by improvement in microphysical properties) providing more reliable weather predictions and climatic simulations.

Data availability. The data is available upon contacting the corresponding author (pedro.jimenezguerrero@um.es)

Author contributions. LP-P wrote the manuscript, with contributions from PJ-G. LP-P and PS designed the experiments; LP-P conducted the numerical simulations and compiled all the experiments, with the support of RL-P. LP-P did the analysis, with the support of PS, RL-P and PJ-G.

Competing interests. The authors declare no conflict of interest.

Acknowledgements. The authors acknowledge the ACEX-CGL2017-87921-R project, funded by the Spanish Ministry of the Economy and Competitiveness and the European Regional Development Fund (ERDF/FEDER). L. P.-P. thanks the FPU14/05505 scholarship from the Spanish Ministry of Education, Culture and Sports and the ERASMUS+ program. P.S. acknowledges funding from the European Research Council (ERC) project constRaining the EffeCts of Aerosols on Precipitation (RECAP) under the European Union's Horizon 2020 research and innovation programme with grant agreement 724602.

References

Ackermann, I. J., Hass, H., Memmesheimer, M., Ebel, A., Binkowski, F. S., and Shankar, U.: Modal aerosol dynamics model for Europe: Development and first applications, Atmospheric Environment, 32, 2981 – 2999, doi: 10.1016/S1352-2310(98)00006-5, 1998.

Ahmadov, R., McKeen, S. A., Robinson, A. L., Bahreini, R., Middlebrook, A. M., de Gouw, J. A., Meagher, J., Hsie, E.-Y., Edgerton, E., Shaw, S., and Trainer, M.: A volatility basis set model for summertime secondary organic aerosols over the eastern United States in 2006, Journal of Geophysical Research: Atmospheres, 117, D06 301, doi: 10.1029/2011JD016831, 2012.

Altaratz, O., Bar-Or, R. Z., Wollner, U., and Koren, I.: Relative humidity and its effect on aerosol optical depth in the vicinity of convective clouds, Environmental Research Letters, 8, 034 025, doi: 10.1088/1748-9326/8/3/034025, 2013.

Andreae, M. O. and Merlet, P.: Emission of trace gases and aerosols from biomass burning, Global Biogeochemical Cycles, 15, 955 – 966, doi: 10.1029/2000GB001382, 2001.

Balzarini, A., Pirovano, G., Honzak, L., Žabkar, R., Curci, G., Forkel, R., Hirtl, M., San José, R., Tuccella, P., and Grell, G.: WRF-Chem model sensitivity to chemical mechanisms choice in reconstructing aerosol optical properties, Atmospheric Environment, 115, 604 – 619, doi: 10.1016/j.atmosenv.2014.12.033, 2015.

Baró, R., Lorente-Plazas, R., Montávez, J. P., and Jiménez-Guerrero, P.: Biomass burning aerosol impact on surface winds during the 2010 Russian heat wave, Geophysical Research Letters, 44, 1088 – 1094, doi: 10.1002/2016GL071484, 2017.

Barriopedro, D., Fischer, E. M., Luterbacher, J., Trigo, R. M., and García-Herrera, R.: The Hot Summer of 2010: Redrawing the Temperature Record Map of Europe, Science, 332, 220 – 224, doi: 10.1126/science.1201224, 2011.

Binkowski, F. S. and Shankar, U.: The regional particulate matter model: 1. Model description and preliminary results, Journal of Geophysical Research: Atmospheres, 100, 26 191 – 26 209, doi: 10.1029/95JD02093, 1995.

Bollasina, M. A., Ming, Y., and Ramaswamy, V.: Earlier onset of the Indian monsoon in the late twentieth century: The role of anthropogenic aerosols, Geophysical Research Letters, 40, 3715–3720, https://doi.org/10.1002/grl.50719, 2013.

Bondur, V.: Satellite monitoring of wildfires during the anomalous heat wave of 2010 in Russia, Izvestiya, Atmospheric and Oceanic Physics, 47, 1039 – 1048, doi: 10.1134/S0001433811090040, 2011.

Booth, B. B. B., Dunstone, N. J., Halloran, P. R., Andrews, T., and Bellouin, N.: Aerosols implicated as a prime driver of twentieth-century North Atlantic climate variability, Nature, 484, 228–232, https://doi.org/10.1038/nature10946, 2012.

Boucher, O.: Atmospheric Aerosols: Properties and Climate Impacts, Springer Netherlands, xVII, 311 pages, doi: 10.1007/978-94-017-9649-1, 2015.

Boucher, O., Randall, D., Artaxo, P., Bretherton, C., Feingold, G., Forster, P., Kerminen, V.-M., Kondo, Y., Liao, H., Lohmann, U., Rasch, P., Satheesh, S., Sherwood, S., Stevens, B., and Zhang, X.: Clouds and aerosols, in: Climate Change 2013: The Physical Science Basis. Contribution of Working Group I to the Fifth Assessment Report of the Intergovernmental Panel on Climate Change, edited by Stocker, T., Qin, D., Plattner, G.-K., Tignor, M., Allen, S., Boschung, J., Nauels, A., Xia, Y., Bex, V., , and Midgley, P., pp. 571 – 657, Cambridge University Press, Cambridge University Press, Cambridge, United Kingdom and New York, NY, USA., 2013.

Brunner, D., Savage, N., Jorba, O., Eder, B., Giordano, L., Badia, A., Balzarini, A., Baró, R., Bianconi, R., Chemel, C., Curci, G., Forkel, R., Jiménez-Guerrero, P., Hirtl, M., Hodzic, A., Honzak, L., Im, U., Knote, C., Makar, P., Manders-Groot, A., van Meijgaard, E., Neal, L., Pérez, J. L., Pirovano, G., San José, R., Schröder, W., Sokhi, R. S., Syrakov, D., Torian, A., Tuccella, P., Werhahn, J., Wolke, R., Yahya, K., Zabkar, R., Zhang, Y., Hogrefe, C., and Galmarini, S.: Comparative analysis of meteorological per-

formance of coupled chemistry-meteorology models in the context of AQMEII phase 2, Atmospheric Environment, 115, 470–498, https://doi.org/10.1016/j.atmosenv.2014.12.032, 2015.

Charlson, R. J., Schwartz, S. E., Hales, J. M., Cess, R. D., Coakley, J. A., Hansen, J. E., and Hofmann, D. J.: Climate Forcing by Anthropogenic Aerosols, Science, 255, 423 – 430, doi: 10.1126/science.255.5043.423, 1992.

Chubarova, N., Nezval', Y., Sviridenkov, I., Smirnov, A., and Slutsker, I.: Smoke aerosol and its radiative effects during extreme fire event over Central Russia in summer 2010, Atmospheric Measurement Techniques, 5, 557 – 568, doi: 10.5194/amt-5-557-2012, 2012.

Claquin, T., Schulz, M., Balkanski, Y., and Boucher, O.: Uncertainties in assessing radiative forcing by mineral dust, Tellus B, 50, 491 – 505, doi: 10.1034/j.1600-0889.1998.t01-2-00007.x, 1998.

Croft, B., Pierce, J. R., Martin, R. V., Hoose, C., and Lohmann, U.: Uncertainty associated with convective wet removal of entrained aerosols in a global climate model, Atmospheric Chemistry and Physics, 12, 10 725–10 748, https://doi.org/10.5194/acp-12-10725-2012, 2012.

Curci, G., Alyuz, U., Baró, R., Bianconi, R., Bieser, J., Christensen, J. H., Colette, A., Farrow, A., Francis, X., Jiménez-Guerrero, P., Im, U., Liu, P., Manders, A., Palacios-Peña, L., Prank, M., Pozzoli, L., Sokhi, R., Solazzo, E., Tuccella, P., Unal, A., Vivanco, M. G., Hogrefe, C., and Galmarini, S.: Modelling black carbon absorption of solar radiation: combining external and internal mixing assumptions, Atmospheric Chemistry and Physics, 19, 181 – 204, doi: 10.5194/acp-19-181-2019, 2019.

Devenish, B. J., Furtado, K., and Thomson, D. J.: Analytical Solutions of the Supersaturation Equation for a Warm Cloud, Journal of the Atmospheric Sciences, 73, 3453–3465, https://doi.org/10.1175/JAS-D-15-0281.1, 2016.

Diapouli, E., Popovicheva, O., Kistler, M., Vratolis, S., Persiantseva, N., Timofeev, M., Kasper-Giebl, A., and Eleftheriadis, K.: Physico-chemical characterization of aged biomass burning aerosol after long-range transport to Greece from large scale wildfires in Russia and surrounding regions, Summer 2010, Atmospheric Environment, 96, 393 – 404, doi: 10.1016/j.atmosenv.2014.07.055, 2014.

Doherty, R. M., Stevenson, D. S., Collins, W. J., and Sanderson, M. G.: Influence of convective transport on tropospheric ozone and its precursors in a chemistry-climate model, Atmospheric Chemistry and Physics, 5, 3205 – 3218, doi: 10.5194/acp-5-3205-2005, 2005.

Easter, R. C., Ghan, S. J., Zhang, Y., Saylor, R. D., Chapman, E. G., Laulainen, N. S., Abdul-Razzak, H., Leung, L. R., Bian, X., and Zaveri, R. A.: MIRAGE: Model description and evaluation of aerosols and trace gases, Journal of Geophysical Research: Atmospheres, 109, D20 210, doi: 10.1029/2004JD004571, 2004.

Eck, T. F., Holben, B. N., Reid, J. S., Dubovik, O., Smirnov, A., O'Neill, N. T., Slutsker, I., and Kinne, S.: Wavelength dependence of the optical depth of biomass burning, urban, and desert dust aerosols, Journal of Geophysical Research: Atmospheres, 104, 31 333 – 31 349, doi: 10.1029/1999JD900923, 1999.

Fast, J. D., Gustafson Jr., W. I., Easter, R. C., Zaveri, R. A., Barnard, J. C., Chapman, E. G., Grell, G. A., and Peckham, S. E.: Evolution of ozone, particulates, and aerosol direct radiative forcing in the vicinity of Houston using a fully coupled meteorology-chemistry-aerosol model, Journal of Geophysical Research: Atmospheres, 111, D21 305, doi: 10.1029/2005JD006721, 2006.

Fernald, F. G., Herman, B. M., and Reagan, J. A.: Determination of Aerosol Height Distributions by Lidar, Journal of Applied Meteorology, 11, 482 – 489, https://doi.org/10.1175/1520-0450(1972)011<0482:DOAHDB>2.0.CO;2, 1972.

Forkel, R., Balzarini, A., Baró, R., Bianconi, R., Curci, G., Jiménez-Guerrero, P., Hirtl, M., Honzak, L., Lorenz, C., Im, U., Pérez, J. L., Pirovano, G., San José, R., Tuccella, P., Werhahn, J., and Žabkar, R.: Analysis of the WRF-Chem contributions to AQMEII phase2 with respect to aerosol radiative feedbacks on meteorology and pollutant distributions, Atmospheric Environment, 115, 630 – 645, doi: 10.1016/j.atmosenv.2014.10.056, 2015.

Forkel, R., Brunner, D., Baklanov, A., Balzarini, A., Hirtl, M., Honzak, L., Jiménez-Guerrero, P., Jorba, O., Pérez, J. L., San José, R., Schöder, W., Tsegas, G., Werhahn, J., Wolke, R., and Žabkar, R.: A Multi-model Case Study on Aerosol Feedbacks in Online Coupled

Chemistry-Meteorology Models Within the COST Action ES1004 EuMetChem, in: Air Pollution Modeling and its Application XXIV. Springer Proceedings in Complexity, pp. 23 – 28, Springer, Cham, 2016.

Forster, P., Ramaswamy, V., Artaxo, P., Berntsen, T., Betts, R., Fahey, D., Haywood, J., Lean, J., Lowe, D., Myhre, G., Nganga, J., Prinn, R., Raga, G., Schulz, M., and Dorland, R. V.: Changes in Atmospheric Constituents and in Radiative Forcing, in: Climate Change 2013: The Physical Science Basis. Contribution of Working Group I to the Fouth Assessment Report of the Intergovernmental Panel on Climate Change, edited by Solomon, S., Qin, D., Manning, M., Chen, Z., Marquis, M., Averyt, K., M.Tignor, and Miller, H., pp. 129 – 234, Cambridge University Press, Cambridge, United Kingdom and New York, NY, USA, 2007.

Galmarini, S., Hogrefe, C., Brunner, D., Makar, P., and Baklanov, A.: Preface, Atmospheric Environment, 115, 340 – 344, doi: 10.1016/j.atmosenv.2015.06.009, 2015.

Geiger, H., Barnes, I., Bejan, I., Benter, T., and Spittler, M.: The tropospheric degradation of isoprene: an updated module for the regional atmospheric chemistry mechanism, Atmospheric Environment, 37, 1503 – 1519, doi: https://doi.org/10.1016/S1352-2310(02)01047-6, 2003.

Ghan, S., Wang, M., Zhang, S., Ferrachat, S., Gettelman, A., Griesfeller, J., Kipling, Z., Lohmann, U., Morrison, H., Neubauer, D., Partridge, D. G., Stier, P., Takemura, T., Wang, H., and Zhang, K.: Challenges in constraining anthropogenic aerosol effects on cloud radiative forcing using present-day spatiotemporal variability, Proceedings of the National Academy of Sciences, 113, 5804–5811, https://doi.org/10.1073/pnas.1514036113, 2016.

Ginoux, P., Horowitz, L. W., Ramaswamy, V., Geogdzhayev, I. V., Holben, B. N., Stenchikov, G., and Tie, X.: Evaluation of aerosol distribution and optical depth in the Geophysical Fluid Dynamics Laboratory coupled model CM2.1 for present climate, Journal of Geophysical Research: Atmospheres, 111, D22 210, doi: 10.1029/2005JD006707, 2006.

Gorchakov, G., Sitnov, S., Sviridenkov, M., Semoutnikova, E., Emilenko, A., Isakov, A., Kopeikin, V., Karpov, A., Gorchakova, I., Verichev, K., Kurbatov, G., and Ponomareva, T.: Satellite and ground-based monitoring of smoke in the atmosphere during the summer wildfires in European Russia in 2010 and Siberia in 2012, International Journal of Remote Sensing, 35, 5698 – 5721, doi: 10.1080/01431161.2014.945008, 2014.

Granier, C., Bessagnet, B., Bond, T., D'Angiola, A., van Der Gon, H. D., Frost, G. J., Heil, A., Kaiser, J. W., Kinne, S., Klimont, Z., et al.: Evolution of anthropogenic and biomass burning emissions of air pollutants at global and regional scales during the 1980–2010 period, Climatic Change, 109, 163 – 190, doi: 10.1007/s10584-011-0154-1, 2011.

Greenfield, S. M.: RAIN SCAVENGING OF RADIOACTIVE PARTICULATE MATTER FROM THE ATMOSPHERE, Journal of Meteorology, 14, 115–125, https://doi.org/10.1175/1520-0469(1957)014<0115:RSORPM>2.0.CO;2, 1957.

Grell, G. A.: Prognostic Evaluation of Assumptions Used by Cumulus Parameterizations, Monthly Weather Review, 121, 764 – 787, doi: 10.1175/1520-0493(1993)121<0764:PEOAUB>2.0.CO;2, 1993.

Grell, G. A. and Dévényi, D.: A generalized approach to parameterizing convection combining ensemble and data assimilation techniques, Geophysical Research Letters, 29, doi: 10.1029/2002GL, 2002.

Grell, G. A. and Freitas, S. R.: A scale and aerosol aware stochastic convective parameterization for weather and air quality modeling, Atmospheric Chemistry and Physics, 14, 5233 – 5250, doi: 10.5194/acp-14-5233-2014, 2014.

Grell, G. A., Dudhia, J., and Stauffer, D. R.: A description of the fifth-generation Penn State/NCAR mesoscale model (MM5), Tech. rep., Mesoscale and Microscale Meteorology Division, National Center for Atmospheric Research, pages 121, doi: 10.5065/D60Z716B, 1994.

Grell, G. A., Peckham, S. E., Schmitz, R., McKeen, S. A., Frost, G., Skamarock, W. C., and Eder, B.: Fully coupled "online" chemistry within the WRF model, Atmospheric Environment, 39, 6957 – 6975, doi: 10.1016/j.atmosenv.2005.04.027, 2005.

Haywood, J. and Boucher, O.: Estimates of the direct and indirect radiative forcing due to tropospheric aerosols: A review, Reviews of Geophysics, 38, 513 – 543, doi: 10.1029/1999RG000078, 2000.

Hong, S.-Y., Noh, Y., and Dudhia, J.: A New Vertical Diffusion Package with an Explicit Treatment of Entrainment Processes, Monthly Weather Review, 134, 2318 – 2341, doi: 10.1175/MWR3199.1, 2006.

Iacono, M. J., Delamere, J. S., Mlawer, E. J., Shephard, M. W., Clough, S. A., and Collins, W. D.: Radiative forcing by long-lived greenhouse gases: Calculations with the AER radiative transfer models, Journal of Geophysical Research: Atmospheres, 113, D13 103, doi: 10.1029/2008JD009944, 2008.

Im, U., Bianconi, R., Solazzo, E., Kioutsioukis, I., Badia, A., Balzarini, A., Baró, R., Bellasio, R., Brunner, D., Chemel, C., Curci, G., Flemming, J., Forkel, R., Giordano, L., Jiménez-Guerrero, P., Hirtl, M., Hodzic, A., Honzak, L., Jorba, O., Knote, C., Kuenen, J. J., Makar, P. A., Manders-Groot, A., Neal, L., Pérez, J. L., Pirovano, G., Pouliot, G., Jose, R. S., Savage, N., Schroder, W., Sokhi, R. S., Syrakov, D., Torian, A., Tuccella, P., Werhahn, J., Wolke, R., Yahya, K., Žabkar, R., Zhang, Y., Zhang, J., Hogrefe, C., and Galmarini, S.: Evaluation of operational on-line-coupled regional air quality models over Europe and North America in the context of AQMEII phase 2. Part I: Ozone, Atmospheric Environment, 115, 404 – 420, doi: 10.1016/j.atmosenv.2014.09.042, 2015a.

Im, U., Bianconi, R., Solazzo, E., Kioutsioukis, I., Badia, A., Balzarini, A., Baró, R., Bellasio, R., Brunner, D., Chemel, C., Curci, G., van der Gon, H. D., Flemming, J., Forkel, R., Giordano, L., Jiménez-Guerrero, P., Hirtl, M., Hodzic, A., Honzak, L., Jorba, O., Knote, C., Makar, P. A., Manders-Groot, A., Neal, L., Pérez, J. L., Pirovano, G., Pouliot, G., Jose, R. S., Savage, N., Schroder, W., Sokhi, R. S., Syrakov, D., Torian, A., Tuccella, P., Wang, K., Werhahn, J., Wolke, R., Žabkar, R., Zhang, Y., Zhang, J., Hogrefe, C., and Galmarini, S.: Evaluation of operational online-coupled regional air quality models over Europe and North America in the context of AQMEII phase 2. Part II: Particulate matter, Atmospheric Environment, 115, 421 – 441, doi: 10.1016/j.atmosenv.2014.08.072, 2015b.

Inness, A., Baier, F., Benedetti, A., Bouarar, I., Chabrillat, S., Clark, H., Clerbaux, C., Coheur, P., Engelen, R. J., Errera, Q., Flemming, J., George, M., Granier, C., Hadji-Lazaro, J., Huijnen, V., Hurtmans, D., Jones, L., Kaiser, J. W., Kapsomenakis, J., Lefever, K., Leitão, J., Razinger, M., Richter, A., Schultz, M. G., Simmons, A. J., Suttie, M., Stein, O., Thépaut, J.-N., Thouret, V., Vrekoussis, M., Zerefos, C., and the MACC team: The MACC reanalysis: an 8 yr data set of atmospheric composition, Atmospheric Chemistry and Physics, 13, 4073 – 4109, doi: 10.5194/acp-13-4073-2013, 2013.

Kasoar, M., Voulgarakis, A., Lamarque, J.-F., Shindell, D. T., Bellouin, N., Collins, W. J., Faluvegi, G., and Tsigaridis, K.: Regional and global temperature response to anthropogenic SO_2 emissions from China in three climate models, Atmospheric Chemistry and Physics, 16, 9785–9804, https://doi.org/10.5194/acp-16-9785-2016, 2016.

Kim, D., Chin, M., Yu, H., Diehl, T., Tan, Q., Kahn, R. A., Tsigaridis, K., Bauer, S. E., Takemura, T., Pozzoli, L., Bellouin, N., Schulz, M., Peyridieu, S., Chédin, A., and Koffi, B.: Sources, sinks, and transatlantic transport of North African dust aerosol: A multimodel analysis and comparison with remote sensing data, Journal of Geophysical Research: Atmospheres, 119, 6259–6277, https://doi.org/10.1002/2013JD021099, 2014.

Kipling, Z., Stier, P., Johnson, C. E., Mann, G. W., Bellouin, N., Bauer, S. E., Bergman, T., Chin, M., Diehl, T., Ghan, S. J., Iversen, T., Kirkevåg, A., Kokkola, H., Liu, X., Luo, G., van Noije, T., Pringle, K. J., vonÂ Salzen, K., Schulz, M., Seland, Ø., Skeie, R. B., Takemura, T., Tsigaridis, K., and Zhang, K.: What controls the vertical distribution of aerosol? Relationships between process sensitivity in HadGEM3–UKCA and inter-model variation from AeroCom Phase II, Atmospheric Chemistry and Physics, 16, 2221 – 2241, doi: 10.5194/acp-16-2221-2016, 2016.

Koffi, B., Schulz, M., Bréon, F.-M., Dentener, F., Steensen, B. M., Griesfeller, J., Winker, D., Balkanski, Y., Bauer, S. E., Bellouin, N., Berntsen, T., Bian, H., Chin, M., Diehl, T., Easter, R., Ghan, S., Hauglustaine, D. A., Iversen, T., Kirkevåg, A., Liu, X., Lohmann, U.,

Myhre, G., Rasch, P., Seland, O., Skeie, R. B., Steenrod, S. D., Stier, P., Tackett, J., Takemura, T., Tsigaridis, K., Vuolo, M. R., Yoon, J., and Zhang, K.: Evaluation of the aerosol vertical distribution in global aerosol models through comparison against CALIOP measurements: AeroCom phase II results, Journal of Geophysical Research: Atmospheres, 121, 7254–7283, https://doi.org/10.1002/2015JD024639, 2016.

Kong, X., Forkel, R., Sokhi, R. S., Suppan, P., Baklanov, A., Gauss, M., Brunner, D., Baró, R., Balzarini, A., Chemel, C., Curci, G., Jiménez-Guerrero, P., Hirtl, M., Honzak, L., Im, U., Pérez, J. L., Pirovano, G., San José, R., Schlünzen, K. H., Tsegas, G., Tuccella, P., Werhahn, J., Žabkar, R., and Galmarini, S.: Analysis of meteorology-chemistry interactions during air pollution episodes using online coupled models within AQMEII phase-2, Atmospheric Environment, 115, 527 – 540, doi: 10.1016/j.atmosenv.2014.09.020, 2015.

Konovalov, I. B., Beekmann, M., Kuznetsova, I. N., Yurova, A., and Zvyagintsev, A. M.: Atmospheric impacts of the 2010 Russian wildfires: integrating modelling and measurements of an extreme air pollution episode in the Moscow region, Atmospheric Chemistry and Physics, 11, 10 031 – 10 056, doi: 10.5194/acp-11-10031-2011, 2011.

Kramm, G., Beheng, K. D., and Müller, H.: Vertical transport of polydispersed aerosol particles in the atmospheric surface layer, in: Precipitation Scavenging and Atmosphere-Surface Exchange Processes, edited by Schwartz, S. and Slinn, W., vol. 2, pp. 1125 – 1141, Hemisphere New York, 1992.

Kuenen, J. J. P., Visschedijk, A. J. H., Jozwicka, M., and Denier van der Gon, H. A. C.: TNO-MACC_II emission inventory; a multi-year (2003–2009) consistent high-resolution European emission inventory for air quality modelling, Atmospheric Chemistry and Physics, 14, 10 963 – 10 976, doi: 10.5194/acp-14-10963-2014, 2014.

Lacagnina, C., Hasekamp, O. P., Bian, H., Curci, G., Myhre, G., van Noije, T., Schulz, M., Skeie, R. B., Takemura, T., and Zhang, K.: Aerosol single-scattering albedo over the global oceans: Comparing PARASOL retrievals with AERONET, OMI, and AeroCom models estimates, Journal of Geophysical Research: Atmospheres, 120, 9814–9836, https://doi.org/10.1002/2015JD023501, 2015.

Ladino, L., Stetzer, O., Hattendorf, B., Günther, D., Croft, B., and Lohmann, U.: Experimental Study of Collection Efficiencies between Submicron Aerosols and Cloud Droplets, Journal of the Atmospheric Sciences, 68, 1853–1864, https://doi.org/10.1175/JAS-D-11-012.1, 2011.

Lau, W. K. M. and Kim, K.-M.: The 2010 Pakistan Flood and Russian Heat Wave: Teleconnection of Hydrometeorological Extremes, Journal of Hydrometeorology, 13, 392 – 403, doi: 10.1175/JHM-D-11-016.1, 2012.

Lee, L. A., Pringle, K. J., Reddington, C. L., Mann, G. W., Stier, P., Spracklen, D. V., Pierce, J. R., and Carslaw, K. S.: The magnitude and causes of uncertainty in global model simulations of cloud condensation nuclei, Atmospheric Chemistry and Physics, 13, 8879 – 8914, doi: 10.5194/acp-13-8879-2013, 2013.

Makar, P., Gong, W., Hogrefe, C., Zhang, Y., Curci, G., Žabkar, R., Milbrandt, J., Im, U., Balzarini, A., Baró, R., Bianconi, R., Cheung, P., Forkel, R., Gravel, S., Hirtl, M., Honzak, L., Hou, A., Jiménez-Guerrero, P., Langer, M., Moran, M., Pabla, B., Pérez, J., Pirovano, G., José, R. S., Tuccella, P., Werhahn, J., Zhang, J., and Galmarini, S.: Feedbacks between air pollution and weather, part 2: Effects on chemistry, Atmospheric Environment, 115, 499 – 526, doi: 10.1016/j.atmosenv.2014.10.021, 2015a.

Makar, P., Gong, W., Milbrandt, J., Hogrefe, C., Zhang, Y., Curci, G., Žabkar, R., Im, U., Balzarini, A., Baró, R., Bianconi, R., Cheung, P., Forkel, R., Gravel, S., Hirtl, M., Honzak, L., Hou, A., Jiménez-Guerrero, P., Langer, M., Moran, M., Pabla, B., Pérez, J., Pirovano, G., San José, R., Tuccella, P., Werhahn, J., Zhang, J., and Galmarini, S.: Feedbacks between air pollution and weather, Part 1: Effects on weather, Atmospheric Environment, 115, 442 – 469, doi: 10.1016/j.atmosenv.2014.12.003, 2015b.

Mann, G. W., Carslaw, K. S., Reddington, C. L., Pringle, K. J., Schulz, M., Asmi, A., Spracklen, D. V., Ridley, D. A., Woodhouse, M. T., Lee, L. A., Zhang, K., Ghan, S. J., Easter, R. C., Liu, X., Stier, P., Lee, Y. H., Adams, P. J., Tost, H., Lelieveld, J., Bauer, S. E., Tsigaridis, K., van Noije, T. P. C., Strunk, A., Vignati, E., Bellouin, N., Dalvi, M., Johnson, C. E., Bergman, T., Kokkola, H., von Salzen, K., Yu, F.,

Luo, G., Petzold, A., Heintzenberg, J., Clarke, A., Ogren, J. A., Gras, J., Baltensperger, U., Kaminski, U., Jennings, S. G., O'Dowd, C. D., Harrison, R. M., Beddows, D. C. S., Kulmala, M., Viisanen, Y., Ulevicius, V., Mihalopoulos, N., Zdimal, V., Fiebig, M., Hansson, H.-C., Swietlicki, E., and Henzing, J. S.: Intercomparison and evaluation of global aerosol microphysical properties among AeroCom models of a range of complexity, Atmospheric Chemistry and Physics, 14, 4679–4713, https://doi.org/10.5194/acp-14-4679-2014, 2014.

Mielonen, T., Aaltonen, V., Lihavainen, H., Hyvärinen, A.-P., Arola, A., Komppula, M., and Kivi, R.: Biomass Burning Aerosols Observed in Northern Finland during the 2010 Wildfires in Russia, Atmosphere, 4, 17 – 34, doi: 10.3390/atmos4010017, 2013.

Morrison, H., Thompson, G., and Tatarskii, V.: Impact of Cloud Microphysics on the Development of Trailing Stratiform Precipitation in a Simulated Squall Line: Comparison of One- and Two-Moment Schemes, Monthly Weather Review, 137, 991 – 1007, doi: 10.1175/2008MWR2556.1, 2009.

Müller, D., Ansmann, A., Mattis, I., Tesche, M., Wandinger, U., Althausen, D., and Pisani, G.: Aerosol-type-dependent lidar ratios observed with Raman lidar, Journal of Geophysical Research: Atmospheres, 112, https://doi.org/10.1029/2006JD008292, 2007.

Nordling, K., Korhonen, H., Räisänen, P., Alper, M. E., Uotila, P., O'Donnell, D., and Merikanto, J.: Role of climate model dynamics in estimated climate responses to anthropogenic aerosols, Atmospheric Chemistry and Physics, 19, 9969–9987, https://doi.org/10.5194/acp-19-9969-2019, https://www.atmos-chem-phys.net/19/9969/2019/, 2019.

Obiso, V. and Jorba, O.: Aerosol-radiation interaction in atmospheric models: Idealized sensitivity study of simulated short-wave direct radiative effects to particle microphysical properties, Journal of Aerosol Science, 115, 46 – 61, doi: 10.1016/j.jaerosci.2017.10.004, 2018.

Obiso, V., Pandolfi, M., Ealo, M., and Jorba, O.: Impact of aerosol microphysical properties on mass scattering cross sections, Journal of Aerosol Science, 112, 68 – 82, doi: 10.1016/j.jaerosci.2017.03.001, 2017.

Palacios-Peña, L., Baró, R., Guerrero-Rascado, J. L., Alados-Arboledas, L., Brunner, D., and Jiménez-Guerrero, P.: Evaluating the representation of aerosol optical properties using an online coupled model over the Iberian Peninsula, Atmospheric Chemistry and Physics, 17, 277 – 296, doi: 10.5194/acp-17-277-2017, 2017.

Palacios-Peña, L., Baró, R., Baklanov, A., Balzarini, A., Brunner, D., Forkel, R., Hirtl, M., Honzak, L., López-Romero, J. M., Montávez, J. P., Pérez, J. L., Pirovano, G., San José, R., Schröder, W., Werhahn, J., Wolke, R., Žabkar, R., and Jiménez-Guerrero, P.: An assessment of aerosol optical properties from remote-sensing observations and regional chemistry–climate coupled models over Europe, Atmospheric Chemistry and Physics, 18, 5021 – 5043, doi: 10.5194/acp-18-5021-2018, 2018.

Palacios-Peña, L., Jiménez-Guerrero, P., Baró, R., Balzarini, A., Bianconi, R., Curci, G., Landi, T. C., Pirovano, G., Prank, M., Riccio, A., Tuccella, P., and Galmarini, S.: Aerosol optical properties over Europe: an evaluation of the AQMEII Phase 3 simulations against satellite observations, Atmospheric Chemistry and Physics, 19, 2965 – 2990, doi: 10.5194/acp-19-2965-2019, 2019a.

Palacios-Peña, L., Lorente-Plazas, R., Montávez, J. P., and Jiménez-Guerrero, P.: Saharan Dust Modeling Over the Mediterranean Basin and Central Europe: Does the Resolution Matter?, Frontiers in Earth Science, 7, 290, doi: 10.3389/feart.2019.00290, 2019b.

Palacios-Peña, L., Fast, J., and Jiménez-Guerrero, P.: Summertime modelling effects of the aerosol size distribution over the Central Europe and the Mediterranean Basin, Submitted to Atmospheric Chemistry and Physics, 2020.

Pan, X., Chin, M., Gautam, R., Bian, H., Kim, D., Colarco, P. R., Diehl, T. L., Takemura, T., Pozzoli, L., Tsigaridis, K., Bauer, S., and Bellouin, N.: A multi-model evaluation of aerosols over South Asia: common problems and possible causes, Atmospheric Chemistry and Physics, 15, 5903–5928, https://doi.org/10.5194/acp-15-5903-2015, 2015.

Penner, J. E., Andreae, M. O., Annegarn, H., Barrie, L., Feichter, J., Hegg, D., Jayaraman, A., Leaitch, R., Murphy, D., Nganga, J., Pitari, G., et al.: Aerosols, their direct and indirect effects, in: Climate Change 2001: The Scientific Basis. Contribution of Working Group I to the Third Assessment Report of the Intergovernmental Panel on Climate Change, edited by Houghton, J. T., Ding, Y., Griggs, D. J.,

Noguer, M., Linden, P. J. v. d., and Xiaosu, D., pp. 289 – 348, Cambridge University Press, Cambridge University Press, Cambridge, United Kingdom and New York, NY, USA., 2001.

Péré, J. C., Bessagnet, B., Mallet, M., Waquet, F., Chiapello, I., Minvielle, F., Pont, V., and Menut, L.: Direct radiative effect of the Russian wildfires and its impact on air temperature and atmospheric dynamics during August 2010, Atmospheric Chemistry and Physics, 14, 1999 – 2013, doi: 10.5194/acp-14-1999-2014, 2014.

Péré, J. C., Bessagnet, B., Pont, V., Mallet, M., and Minvielle, F.: Influence of the aerosol solar extinction on photochemistry during the 2010 Russian wildfires episode, Atmospheric Chemistry and Physics, 15, 10 983 – 10 998, doi: 10.5194/acp-15-10983-2015, 2015.

Pleim, J., Venkatram, A., and Yamartino, R.: ADOM/TADAP Model Development Program: The Dry Deposition Module, Atmospheric Environment (1967), 14, 1013 – 1016, 1984.

Portin, H., Mielonen, T., Leskinen, A., Arola, A., Pärjälä, E., Romakkaniemi, S., Laaksonen, A., Lehtinen, K., and Komppula, M.: Biomass burning aerosols observed in Eastern Finland during the Russian wildfires in summer 2010 – Part 1: In-situ aerosol characterization, Atmospheric Environment, 47, 269 – 278, doi: 10.1016/j.atmosenv.2011.10.067, 2012.

Pouliot, G., Pierce, T., van der Gon, H. D., Schaap, M., Moran, M., and Nopmongcol, U.: Comparing emission inventories and model-ready emission datasets between Europe and North America for the AQMEII project, Atmospheric Environment, 53, 4 – 14, doi: 10.1016/j.atmosenv.2011.12.041, 2012.

Pouliot, G., van der Gon, H. A. C. D., Kuenen, J., Zhang, J., Moran, M. D., and Makar, P. A.: Analysis of the emission inventories and model-ready emission datasets of Europe and North America for phase 2 of the AQMEII project, Atmospheric Environment, 115, 345 – 360, doi: 10.1016/j.atmosenv.2014.10.061, 2015.

Quan, J., Di, Z., Duan, Q., Gong, W., Wang, C., Gan, Y., Ye, A., and Miao, C.: An evaluation of parametric sensitivities of different meteorological variables simulated by the WRF model, Quarterly Journal of the Royal Meteorological Society, 142, 2925–2934, doi: 10.1002/qj.2885, 2016.

Rahmstorf, S. and Coumou, D.: Increase of extreme events in a warming world, Proceedings of the National Academy of Sciences, 108, 17 905 – 17 909, doi: 10.1073/pnas.1101766108, 2011.

Randall, D. A., Wood, R. A., Bony, S., Colman, R., Fichefet, T., Fyfe, J., Kattsov, V., Pitman, A., Shukla, J., Srinivasan, J., Stouffer, R. J., Sumi, A., and Taylor, K. E.: Climate models and their evaluation, in: Climate Change 2013: The Physical Science Basis. Contribution of Working Group I to the Fouth Assessment Report of the Intergovernmental Panel on Climate Change, edited by Solomon, S., Qin, D., Manning, M., Chen, A., Marquis, M., Averyt, K., Tignor, M., and Miller, H., pp. 589 – 662, Cambridge University Press, Cambridge University Press, Cambridge, United Kingdom and New York, NY, USA., 2007.

Randles, C. A., Kinne, S., Myhre, G., Schulz, M., Stier, P., Fischer, J., Doppler, L., Highwood, E., Ryder, C., Harris, B., Huttunen, J., Ma, Y., Pinker, R. T., Mayer, B., Neubauer, D., Hitzenberger, R., Oreopoulos, L., Lee, D., Pitari, G., Di Genova, G., Quaas, J., Rose, F. G., Kato, S., Rumbold, S. T., Vardavas, I., Hatzianastassiou, N., Matsoukas, C., Yu, H., Zhang, F., Zhang, H., and Lu, P.: Intercomparison of shortwave radiative transfer schemes in global aerosol modeling: results from the AeroCom Radiative Transfer Experiment, Atmospheric Chemistry and Physics, 13, 2347–2379, https://doi.org/10.5194/acp-13-2347-2013, 2013.

Regayre, L. A., Johnson, J. S., Yoshioka, M., Pringle, K. J., Sexton, D. M. H., Booth, B. B. B., Lee, L. A., Bellouin, N., and Carslaw, K. S.: Aerosol and physical atmosphere model parameters are both important sources of uncertainty in aerosol ERF, Atmospheric Chemistry and Physics, 18, 9975–10 006, https://doi.org/10.5194/acp-18-9975-2018, 2018.

Romakkaniemi, S., Arola, A., Kokkola, H., Birmili, W., Tuch, T., Kerminen, V.-M., Räisänen, P., Smith, J. N., Korhonen, H., and Laaksonen, A.: Effect of aerosol size distribution changes on AOD, CCN and cloud droplet concentration: Case studies from Erfurt and Melpitz, Germany, Journal of Geophysical Research: Atmospheres, 117, D07 202, doi: 10.1029/2011JD017091, 2012.

Safronov, A. N., Fokeeva, E. V., Rakitin, V. S., Grechko, E. I., and Shumsky, R. A.: Severe Wildfires Near Moscow, Russia in 2010: Modeling of Carbon Monoxide Pollution and Comparisons with Observations, Remote Sensing, 7, 395 – 429, doi: 10.3390/rs70100395, 2015.

Sarrafzadeh, M., Wildt, J., Pullinen, I., Springer, M., Kleist, E., Tillmann, R., Schmitt, S. H., Wu, C., Mentel, T. F., Zhao, D., Hastie, D. R., and Kiendler-Scharr, A.: Impact of NO_x and OH on secondary organic aerosol formation from β-pinene photooxidation, Atmospheric Chemistry and Physics, 16, 11 237 – 11 248, doi: 10.5194/acp-16-11237-2016, 2016.

Saxena, P., Hudischewskyj, A. B., Seigneur, C., and Seinfeld, J. H.: A comparative study of equilibrium approaches to the chemical characterization of secondary aerosols, Atmospheric Environment (1967), 20, 1471 – 1483, doi: 10.1016/0004-6981(86)90019-3, 1986.

Schaap, M., Roemer, M., Sauter, F., Boersen, G., Timmermans, R., Builtjes, P. J. H., and Vermeulen, A. T.: LOTOS-EUROS: Documentation, Tech. rep., TNO, 57 pages, 2005.

Schimel, D., Alves, D., Enting, I., Heimann, M., Joos, F., Raynaud, D., Wigley, T., Prather, M., Derwent, R., Ehhalt, D., Fraser, P., Sanhuenza, E., Zhou, X., Jonas, P., Charlson, R., Rodhe, H., Sadasivan, S., Shine, K. P., Fouquart, Y., Ramaswamy, V., Solomon, S., Srinivasan, J., Albritton, D., Isaksen, I., Lal, M., and Wuebbles, D.: Radiative forcing of climate change, in: Climate Change 1996, Contribution of Working Group I to the Second Assessment Report of the Intergovernmental Panel on Climate Change, edited by Houghton, J. T., Meira Filho, L. G., Callander, B. A., Harris, N., Kattenberg, A., and Maskell, K., Cambridge University Press, Cambridge, United Kingdom and New York, NY, USA, 1996.

Sedlàček, J., Martius, O., and Knutti, R.: Influence of subtropical and polar sea-surface temperature anomalies on temperatures in Eurasia, Geophysical Research Letters, 38, L12 803, doi: 10.1029/2011GL047764, 2011.

Seinfeld, J. H. and Pandis, S. N.: Atmospheric Chemistry and Physics: From Air Pollution to Climate Change, John Wiley & Sons, INC., Second edn., 1225 pages, 2006.

Slinn, S. and Slinn, W.: Predictions for particle deposition on natural waters, Atmospheric Environment (1967), 14, 1013 – 1016, doi: 10.1016/0004-6981(80)90032-3, 1980.

Soares, J., Sofiev, M., and Hakkarainen, J.: Uncertainties of wild-land fires emission in AQMEII phase 2 case study, Atmospheric Environment, 115, 361 – 370, doi: 10.1016/j.atmosenv.2015.01.068, 2015.

Sofiev, M., Vankevich, R., Lotjonen, M., Prank, M., Petukhov, V., Ermakova, T., Koskinen, J., and Kukkonen, J.: An operational system for the assimilation of the satellite information on wild-land fires for the needs of air quality modelling and forecasting, Atmospheric Chemistry and Physics, 9, 6833 – 6847, doi: 10.5194/acp-9-6833-2009, 2009.

Stier, P., Feichter, J., Kinne, S., Kloster, S., Vignati, E., Wilson, J., Ganzeveld, L., Tegen, I., Werner, M., Balkanski, Y., Schulz, M., Boucher, O., Minikin, A., and Petzold, A.: The aerosol-climate model ECHAM5-HAM, Atmospheric Chemistry and Physics, 5, 1125 – 1156, doi: 10.5194/acp-5-1125-2005, 2005.

Stockwell, W. R., Kirchner, F., Kuhn, M., and Seefeld, S.: A new mechanism for regional atmospheric chemistry modeling, Journal of Geophysical Research: Atmospheres, 102, 25 847 – 25 879, doi: 10.1029/97JD00849, 1997.

Tegen, I. and Lacis, A. A.: Modeling of particle size distribution and its influence on the radiative properties of mineral dust aerosol, Journal of Geophysical Research: Atmospheres, 101, 19 237 – 19 244, doi: 10.1029/95JD03610, 1996.

Tewari, M., Chen, F., Wang, W., Dudhia, J., LeMone, M., Mitchell, K., Ek, M., Gayno, G., Wegiel, J., and Cuenca, R.: Implementation and verification of the unified NOAH land surface model in the WRF model, in: 20th conference on weather analysis and forecasting/16th conference on numerical weather prediction, pp. 11 – 15, 2004.

Toll, V., Reis, K., Ots, R., Kaasik, M., Männik, A., Prank, M., and Sofiev, M.: SILAM and MACC reanalysis aerosol data used for simulating the aerosol direct radiative effect with the NWP model HARMONIE for summer 2010 wildfire case in Russia, Atmospheric Environment, 121, 75 – 85, doi: 10.1016/j.atmosenv.2015.06.007, 2015.

Trenberth, K. E. and Fasullo, J. T.: Climate extremes and climate change: The Russian heat wave and other climate extremes of 2010, Journal of Geophysical Research: Atmospheres, 117, D17 103, doi: 10.1029/2012JD018020, 2012.

Tsigaridis, K., Daskalakis, N., Kanakidou, M., Adams, P. J., Artaxo, P., Bahadur, R., Balkanski, Y., Bauer, S. E., Bellouin, N., Benedetti, A., Bergman, T., Berntsen, T. K., Beukes, J. P., Bian, H., Carslaw, K. S., Chin, M., Curci, G., Diehl, T., Easter, R. C., Ghan, S. J., Gong, S. L., Hodzic, A., Hoyle, C. R., Iversen, T., Jathar, S., Jimenez, J. L., Kaiser, J. W., Kirkevåg, A., Koch, D., Kokkola, H., Lee, Y. H., Lin, G., Liu, X., Luo, G., Ma, X., Mann, G. W., Mihalopoulos, N., Morcrette, J.-J., Müller, J.-F., Myhre, G., Myriokefalitakis, S., Ng, N. L., O'Donnell, D., Penner, J. E., Pozzoli, L., Pringle, K. J., Russell, L. M., Schulz, M., Sciare, J., Seland, Ø., Shindell, D. T., Sillman, S., Skeie, R. B., Spracklen, D., Stavrakou, T., Steenrod, S. D., Takemura, T., Tiitta, P., Tilmes, S., Tost, H., van Noije, T., van Zyl, P. G., von Salzen, K., Yu, F., Wang, Z., Wang, Z., Zaveri, R. A., Zhang, H., Zhang, K., Zhang, Q., and Zhang, X.: The AeroCom evaluation and intercomparison of organic aerosol in global models, Atmospheric Chemistry and Physics, 14, 10 845–10 895, https://doi.org/10.5194/acp-14-10845-2014, 2014.

Tuccella, P., Curci, G., Visconti, G., Bessagnet, B., Menut, L., and Park, R. J.: Modeling of gas and aerosol with WRF/Chem over Europe: Evaluation and sensitivity study, Journal of Geophysical Research: Atmospheres, 117, D03 303, doi: 10.1029/2011JD016302, 2012.

Tuccella, P., Curci, G., Grell, G. A., Visconti, G., Crumeyrolle, S., Schwarzenboeck, A., and Mensah, A. A.: A new chemistry option in WRF-Chem v. 3.4 for the simulation of direct and indirect aerosol effects using VBS: evaluation against IMPACT-EUCAARI data, Geoscientific Model Development, 8, 2749 – 2776, doi: 10.5194/gmd-8-2749-2015, 2015.

van Donkelaar, A., Martin, R. V., Levy, R. C., da Silva, A. M., Krzyzanowski, M., Chubarova, N. E., Semutnikova, E., and Cohen, A. J.: Satellite-based estimates of ground-level fine particulate matter during extreme events: A case study of the Moscow fires in 2010, Atmospheric Environment, 45, 6225 – 6232, doi: https://doi.org/10.1016/j.atmosenv.2011.07.068, 2011.

Villarini, G. and Vecchi, G. A.: Projected Increases in North Atlantic Tropical Cyclone Intensity from CMIP5 Models, Journal of Climate, 26, 3231–3240, 2013.

Žabkar, R., Honzak, L., Skok, G., Forkel, R., Rakovec, J., Ceglar, A., and Žagar, N.: Evaluation of the high resolution WRF-Chem (v3.4.1) air quality forecast and its comparison with statistical ozone predictions, Geoscientific Model Development, 8, 2119 – 2137, doi: 10.5194/gmd-8-2119-2015, 2015.

Weigum, N., Schutgens, N., and Stier, P.: Effect of aerosol subgrid variability on aerosol optical depth and cloud condensation nuclei: implications for global aerosol modelling, Atmospheric Chemistry and Physics, 16, 13 619 – 13 639, doi: 10.5194/acp-16-13619-2016, 2016.

Wesely, M. L.: Parameterization of surface resistances to gaseous dry deposition in regional-scale numerical models, Atmospheric Environment (1967), 23, 1293 – 1304, doi: 10.1016/0004-6981(89)90153-4, 1989.

Wiedinmyer, C., Akagi, S. K., Yokelson, R. J., Emmons, L. K., Al-Saadi, J. A., Orlando, J. J., and Soja, A. J.: The Fire INventory from NCAR (FINN): a high resolution global model to estimate the emissions from open burning, Geoscientific Model Development, 4, 625 – 641, doi: 10.5194/gmd-4-625-2011, 2011.

Witte, J. C., Douglass, A. R., da Silva, A., Torres, O., Levy, R., and Duncan, B. N.: NASA A-Train and Terra observations of the 2010 Russian wildfires, Atmospheric Chemistry and Physics, 11, 9287 – 9301, doi: 10.5194/acp-11-9287-2011, 2011.

Wong, D. C., Pleim, J., Mathur, R., Binkowski, F., Otte, T., Gilliam, R., Pouliot, G., Xiu, A., Young, J. O., and Kang, D.: WRF-CMAQ two-way coupled system with aerosol feedback: software development and preliminary results, Geoscientific Model Development, 5, 299 – 312, doi: 10.5194/gmd-5-299-2012, 2012.

Wooster, M. J., Roberts, G., Perry, G. L. W., and Kaufman, Y. J.: Retrieval of biomass combustion rates and totals from fire radiative power observations: FRP derivation and calibration relationships between biomass consumption and fire radiative energy release, Journal of Geophysical Research: Atmospheres, 110, D24 311, doi: 10.1029/2005JD006318, 2005.

Yoon, S.-C. and Kim, J.: Influences of relative humidity on aerosol optical properties and aerosol radiative forcing during ACE-Asia, Atmospheric Environment, 40, 4328 – 4338, doi: 10.1016/j.atmosenv.2006.03.036, 2006.

Yoshioka, M., Regayre, L. A., Pringle, K. J., Johnson, J. S., Mann, G. W., Partridge, D. G., Sexton, D. M. H., Lister, G. M. S., Schutgens, N., Stier, P., Kipling, Z., Bellouin, N., Browse, J., Booth, B. B. B., Johnson, C. E., Johnson, B., Mollard, J. D. P., Lee, L., and Carslaw, K. S.: Ensembles of Global Climate Model Variants Designed for the Quantification and Constraint of Uncertainty in Aerosols and Their Radiative Forcing, Journal of Advances in Modeling Earth Systems, 11, 3728–3754, https://doi.org/10.1029/2019MS001628, 2019.

Zhang, K., O'Donnell, D., Kazil, J., Stier, P., Kinne, S., Lohmann, U., Ferrachat, S., Croft, B., Quaas, J., Wan, H., Rast, S., and Feichter, J.: The global aerosol-climate model ECHAM-HAM, version 2: sensitivity to improvements in process representations, Atmospheric Chemistry and Physics, 12, 8911 – 8949, doi: 10.5194/acp-12-8911-2012, 2012.

Zvyagintsev, A. M., Blum, O. B., Glazkova, A. A., Kotel'nikov, S. N., Kuznetsova, I. N., Lapchenko, V. A., Lezina, E. A., Miller, E. A., Milyaev, V. A., Popikov, A. P., Semutnikova, E. G., TarasovaI, O. A., and Shalygina, Y.: Anomalies of trace gases in the air of the European part of Russia and Ukraine in summer 2010, Atmospheric and Oceanic Optics, 24, 536 – 542, doi: 10.1134/S1024856011060145, 2011.

Table 1. WRF-Chem physical and chemical configuration used in the sensitivity tests.

Scheme	Option	Reference
Physic		
Microphysics	Morrison	Morrison et al. (2009)
SW & LW radiation	RRTM	Iacono et al. (2008)
Planetary boundary layer	YSU	Hong et al. (2006)
Cumulus	Grell-Freitas	Grell and Freitas (2014)
Soil	Noah	Tewari et al. (2004)
Chemistry		
Gas-phase	RACM-KPP	Stockwell et al. (1997) Geiger et al. (2003)
Aerosol	MADE/VBS	Ackermann et al. (1998) Tuccella et al. (2015)
Photolysis	Fast-J	Fast et al. (2006)
Dry Deposition		Wesely (1989)
Wet Deposition	grid-scale	
ARI & ACI	ON	

Table 2. Description of the experiments carried out to perform the sensitivity tests of aerosol to different processes; changes of relative humidity (RH), dry deposition (DDV), convective transport and wet scavenging.

Experiment	Description
Base Case	–
L10RH	RH scaled to 0.9 in the aerosol module
H05RH	RH scaled to 1.005 in the aerosol module
H1RH	RH scaled to 1.01 in the aerosol module
NO_DD	No aerosol dry deposition (DD)
LDDV_AIT	DDV scaled to 0.5 for Aitken Mode
HDDV_AIT	DDV scaled to 2 for Aitken Mode
LDDV_ACC	DDV scaled to 0.1 for the Accumulation Mode
HDDV_ACC	DDV scaled to 10 for the Accumulation Mode
NO_CONV_TR	No sub-grid convective transport
LCONV_TR	Sub-grid convective transport scaled to 0.5
HCONV_TR	Sub-grid convective transport scaled to 1.5
NO_WS	No stratiform wet scavenging

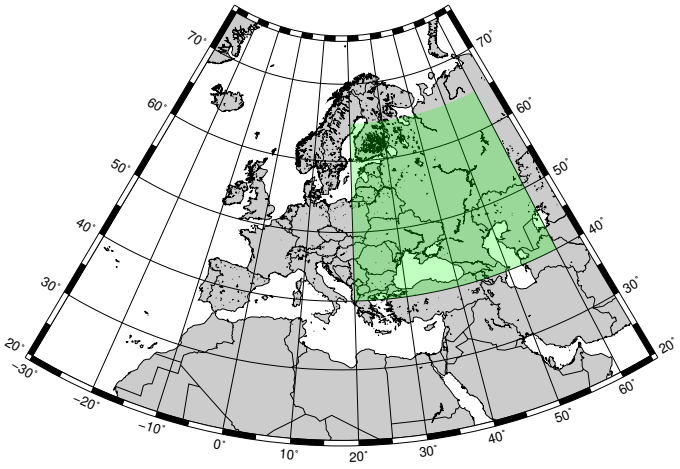

Figure 1. Simulated domain (grey) and fire-affected target area (green box).

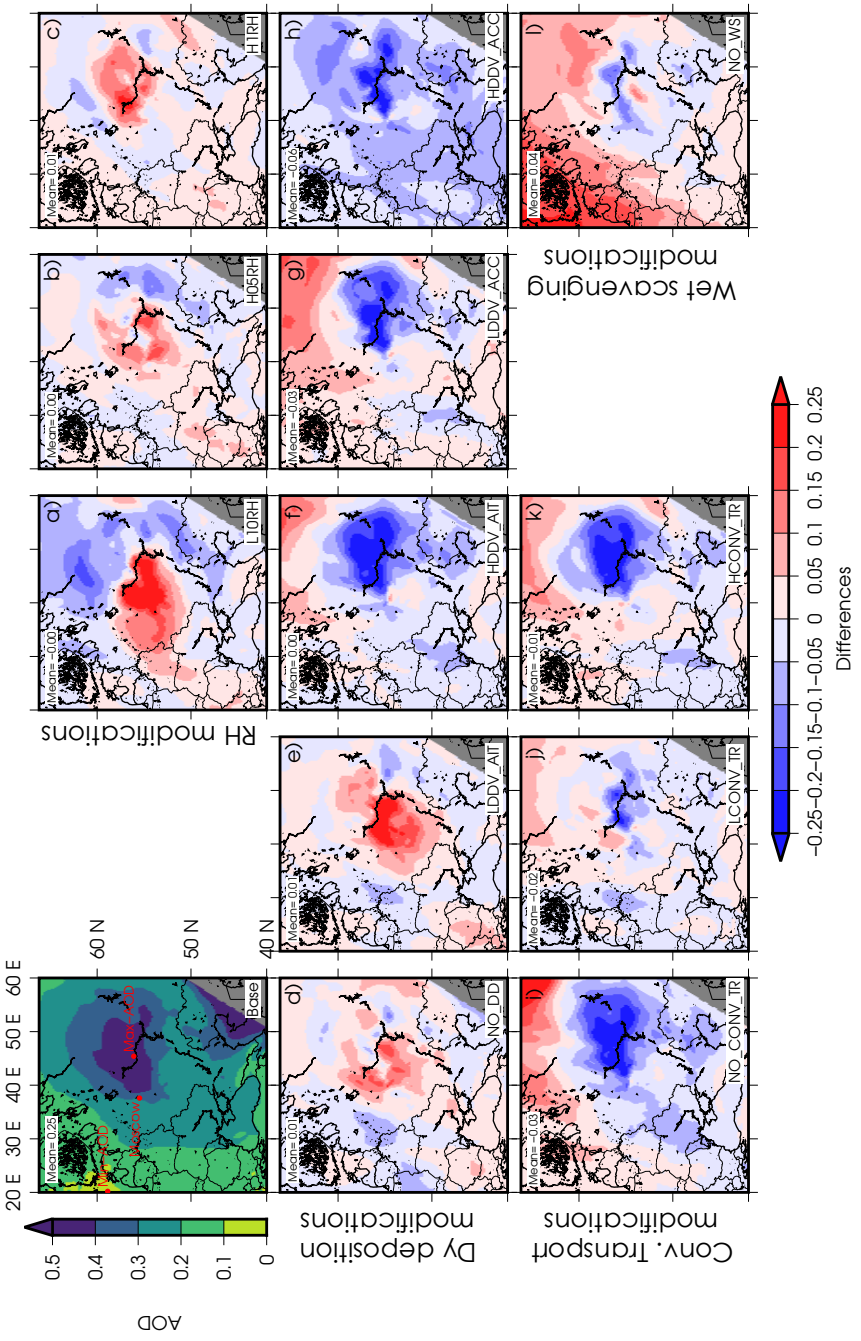

Figure 2. Modelled AOD at 550 nm for the base case (top-left) and mean ~~relative~~ bias differences between experiments and the base case. RH modifications at the top-right: a) scaled to 0.9 (L10RH); b) scaled to 1.005 (H05RH); and c) scaled to 1.01 (H1RH). Dry deposition modifications at the second row: d) the suppression (NO_DD); e) the low DDV for the Aitken mode (LDDV_AIT); f) the high (HDDV_AIT); g) the low DDV for the Accumulation mode (LDDV_ACC); and h) the high (HDDV_ACC). Sub-grid convective transport are in bottom-right row: i) the suppression (NO_CONV_TRANS); j) scaled to 0.5 (LCONV_TRANS) and k) scaled to 1.5 (HCONV_TRANS). Bottom-left panel, l), is the suppression of the wet scavenging.

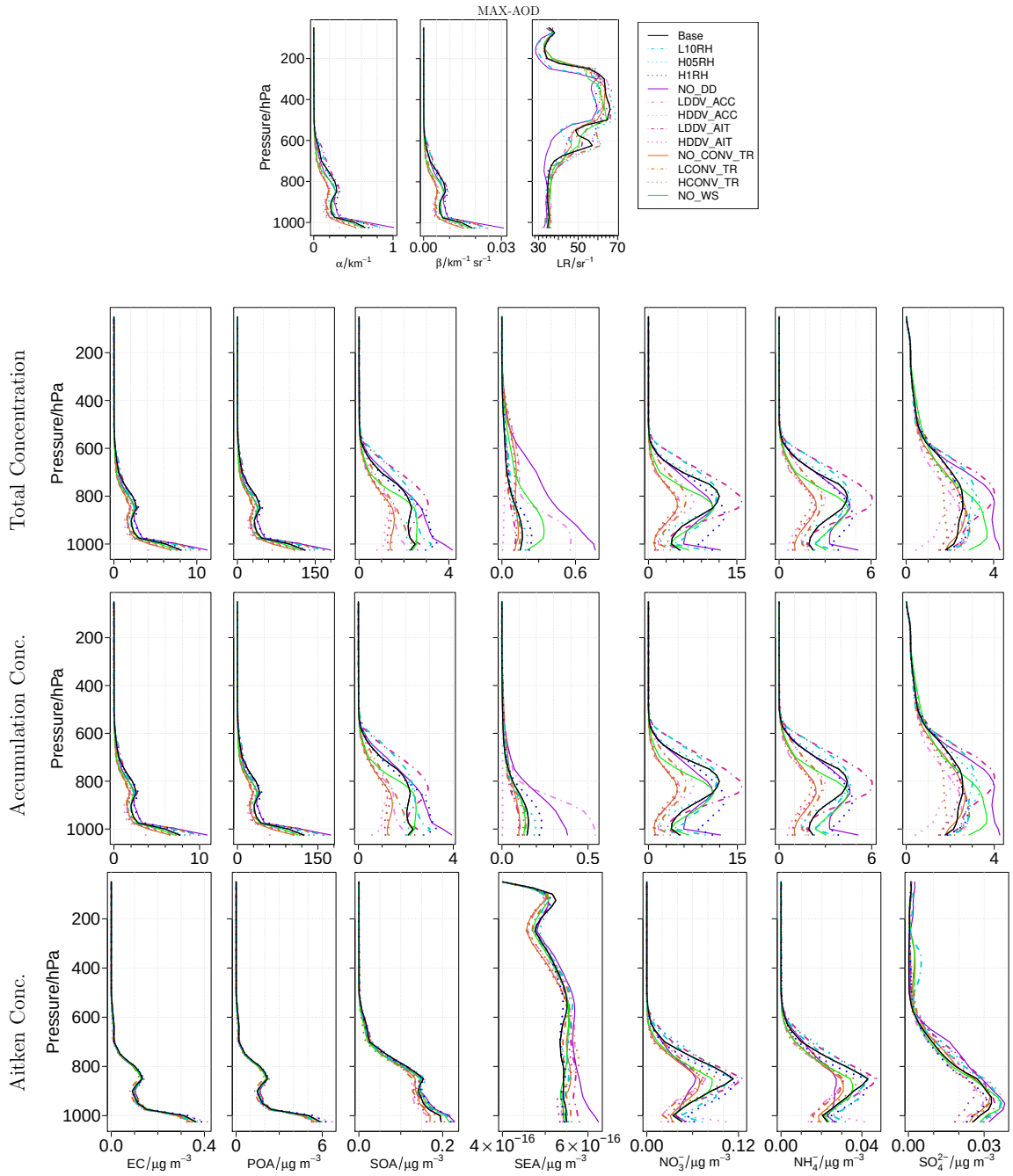

Figure 3. Profiles over the Max-AOD location. Top row shows the α (left), β (centre) & LR (right). From second to bottom rows, columns display concentration of EC, POA,SOA, SEA, NO_3^-, NH_4^- & SO_4^{2-}. The second row is for total concentration; the third for dry; and the bottom for wet. The solid black line represents the base case. The blue color is for RH sensitivity: the dotted dark is the high in 1 % (H1RH); the dotted light, the high in 0.5 % (H05RH); and the dotted-dashed light, the low in 10 % (L10RH). The violet color is for dry deposition. The solid dark is the no dry deposition (NO_DD). The rest dark are for the modification of DDV in the Aitken mode: the dotted is the high (HDDV_AIT); and the dotted-dashed, the low (LDDV_AIT). Similar but in light violet is for the accumulation mode: the dotted is the high (HDDV_ACC); and the dotted-dashed, the low (DDV_ACC). The brown color is for sub-grid convective transport: the solid, without it (NO_CONV_TR); the dotted, the high case (HCONC_TR); and the dotted-dashed, the low (LCONV_TR). The solid green represents the wet scavenging turned off (NO_WS).

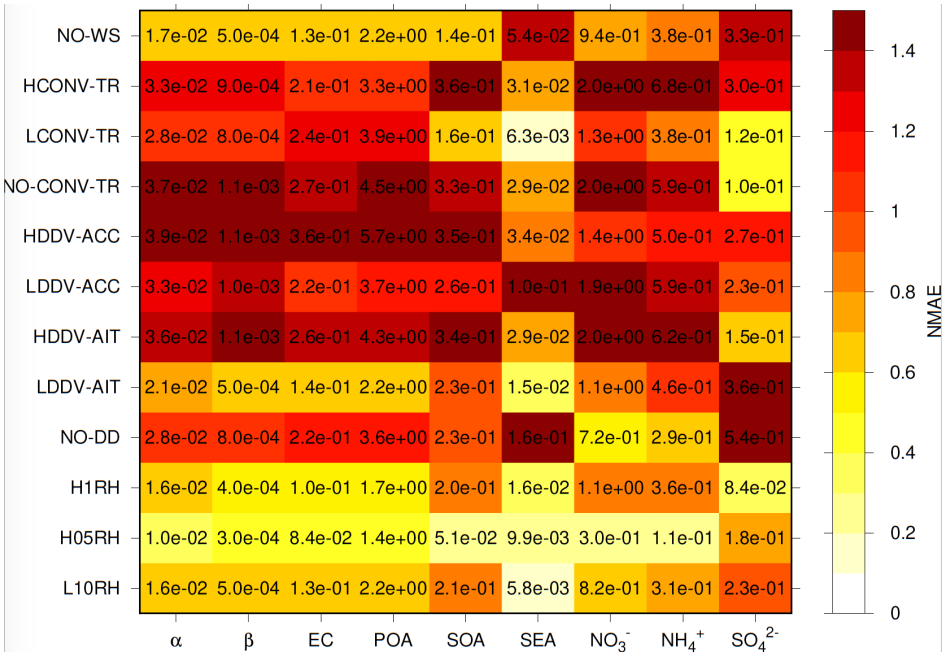

Figure 4. Normalized absolute differences (color) and absolute differences (numbers) between each experiment and the base case over the MAX-AOD location. Columns represent each variable and rows each experiment.

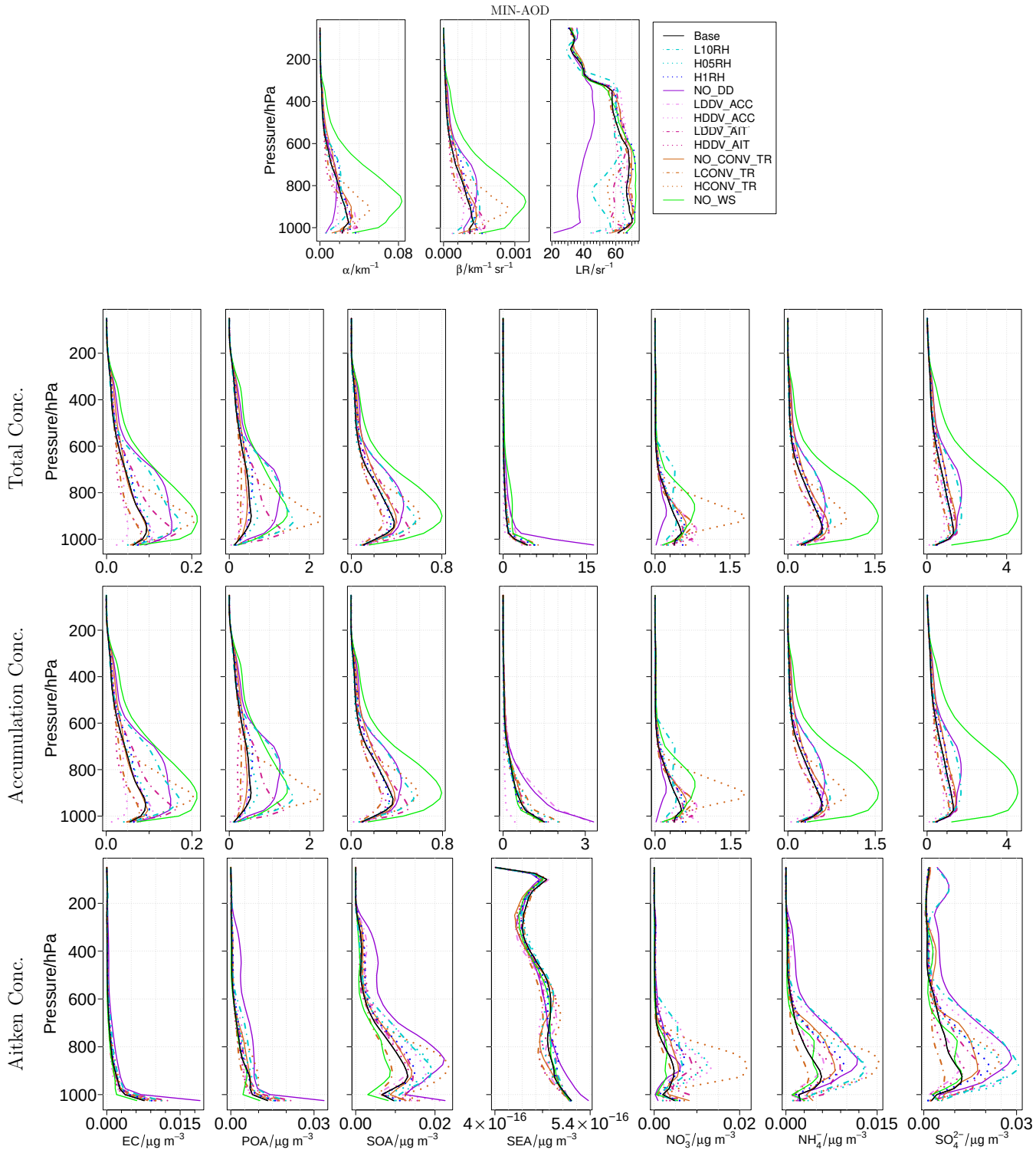

Figure 5. As Figure 3 but over the MIN-AOD location.

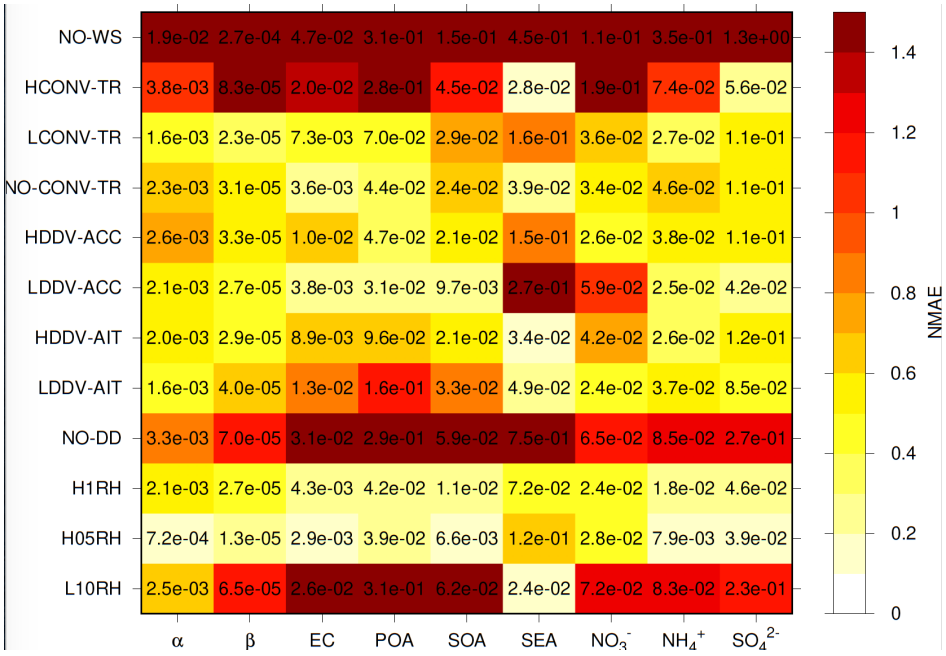

Figure 6. As Figure 4 but over MIN-AOD location.

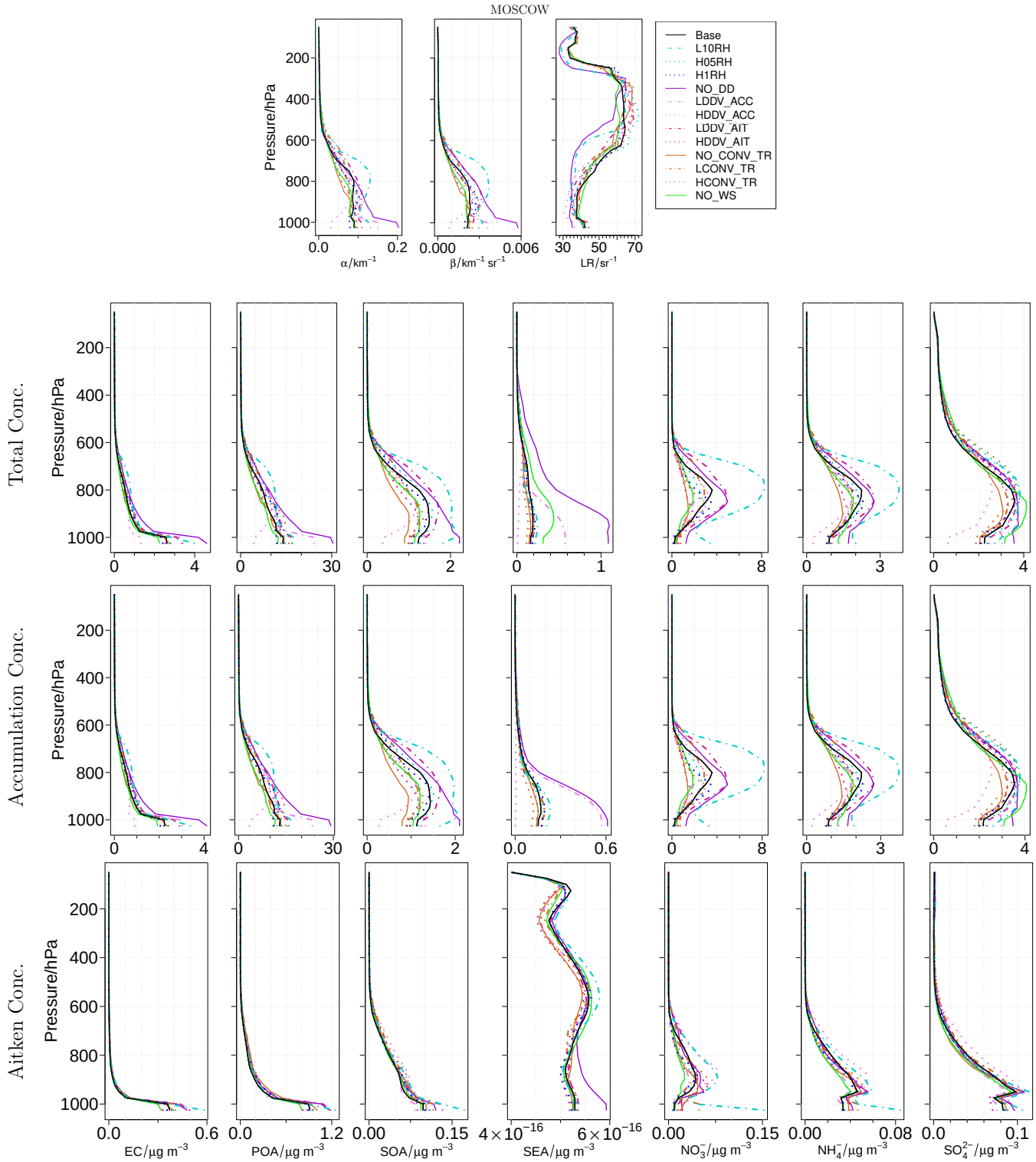

Figure 7. As Figure 3 but over the Moscow location.

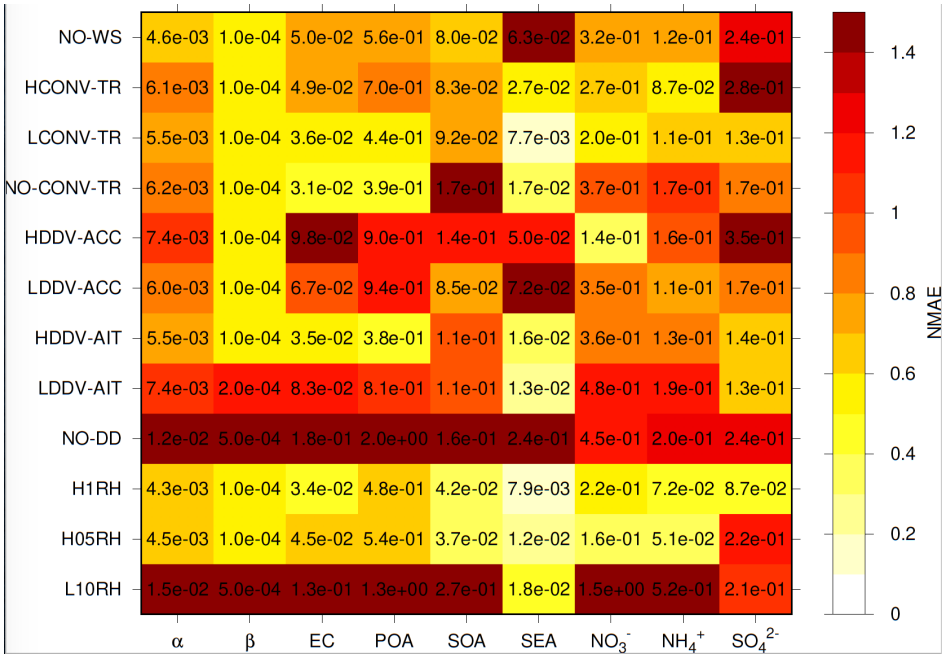

Figure 8. As Figure 4 but over Moscow location.